INTERFACE SCIENCE 3, 241–267 (1996)

Solute Segregation at Grain Boundaries

SIEGFRIED HOFMANN*
Max-Planck-Institut für Metallforschung, Institut für Werkstoffwissenschaft, Seestraße 92, D-70174 Stuttgart, Germany

PAVEL LEJČEK
Institute of Physics, Academy of Sciences of the Czech Republic, Na Slovance 2, CZ-180 40 Prague 8, Czech Republic

Received ; Revised

Abstract. This feature article summarizes the present art and science of grain boundary segregation from the viewpoint of the authors activities in this field. In the part on equilibrium segregation, fundamental effects on grain boundary segregation are discussed such as the nature of the solute/matrix binary system, presence of additional elements, temperature, grain boundary orientation and type of interface. In addition, the predictive capabilities of grain boundary segregation diagrams are outlined. The present models of segregation kinetics are reviewed and discussed in connection with recent experiments. The last part of the paper is focussed on the most important consequences of grain boundary segregation, i.e., grain boundary cohesion and fracture.

Keywords: grain boundary segregation, grain boundary cohesion, fracture, kinetics, equilibrium, anisotropy

1. Introduction

Practical experience of many centuries has led to the common knowledge that low additions of specific impurities to a material substantially change its mechanical properties such as strength and ductility. The existence of grain boundaries in solids has been known for more than a hundred years. However, only several decades ago the first experiments appeared which indicated indirectly that this change in mechanical behavior is closely related to *solute segregation at grain boundaries*, thus showing these interfaces to be a weak link of the materials structure. An intensive study of grain boundary segregation and its role in changing many mechanical and physical properties started in the 1970s and was enhanced by the development of surface analysis techniques, in particular Auger electron spectroscopy. Since that time, considerable progress has been achieved in understanding the phenomenon of grain boundary segregation. It is now well recognized that solute or impurity segregation substantially affects the basic physicochemical properties of grain boundaries, e.g., their energetics, kinetics, cohesion, mobility and electrochemical behavior, and through them many related materials properties such as stress relief cracking, creep embrittlement, recrystallization, diffusion creep, temper brittlenes, hydrogen and liquid metal embrittlement, intergranular corrosion, stress corrosion cracking, and sintering [1].

The boom of experimental studies in the 1970s led to related theoretical studies. During that time, solute segregation was measured mainly in polycrystals of various engineering materials as well as in model alloys. These measurements provided good estimates of segregation behavior and, in many cases, values of the thermodynamic parameters. Since the results obtained from measurements in polycrystals

*Present address: National Research Institute for Metals, 1-2-1 Sengen, Tsukuba, Ibaraki 305, Japan, Fax: +81 298 53 1093.

represent the composition averaged over a number of unknown grain boundaries, the corresponding values of segregation enthalpy and entropy are of rather limited physical meaning. The improved sensitivity of surface analysis techniques and particularly the possibility to study individual, crystallographically well-characterized grain boundaries in oriented bicrystals in the 1980s represent the first step how to overcome this drawback. Later, other techniques such as atom–probe field ion microscopy and more recently high-resolution transmission electron microscopy led to considerable progress in understanding the mechanisms of solute segregation at individual sites at selected grain boundaries. Simultaneously with this experimental research on solute segregation, large effort has been spent since the 1980s in theoretical studies of chemical composition of grain boundaries by means of computer simulations. Studies combining observation of segregated grain boundaries by high-resolution and analytical electron microscopy and its computer simulation are expected to be a highly promising approach in the future [2].

Different phenomena may be understood by the term *grain boundary segregation*:

1) equilibrium distribution of solutes between boundary and bulk governed by the minimum of the total free energy of the whole system at a given temperature,
2) the kinetics of the process to attain the equilibrium solute distribution at a grain boundary, and
3) non-equilibrium solute distribution induced by some external effects, e.g., quenching, stressing, radiation, grain boundary movement, and growth of precipitates.

A huge number of papers concerning various aspects of grain boundary segregation were published in the past decades, including many review papers and books. Papers [3–23] as well as our very recent surveys [1, 2] can serve as fundamental examples. Our research during the last two decades was focussed mainly on the former two items, i.e., on the equilibrium segregation and on the kinetics of this process. In addition, we often studied solute segregation at free surfaces for a comparison to the beahavior of grain boundaries. In the present feature article we summarize the results of this research in context with the current art and science of grain boundary segregation, and critically review some of the recent advances.

2. Equilibrium Segregation

In general, solute segregation can be considered as the result of an interaction between a "chemical" defect (foreign atom in an otherwise homogeneous bulk) and a structural defect[1] of a material. The driving force for this process is usually defined as the difference of the free energy between two states (i) a foreign atom in a configuration with a structural defect, and (ii) the same atom dissolved in the bulk [15]. Due to the general similarity of the above mentioned interaction for different kinds of structural defects, particular types of solute segregation can be described in the same phenomenological manner irrespective of some necessary refinement in individual cases. For example, the theories of gas adsorption at liquid or solid surfaces could successfully be used and adapted to describe grain boundary segregation [24].

A general theory of interfacial segregation was developed by Guttmann in the 1970s on the basis of thermodynamic description of distribution of different types of species between two phases, i.e., bulk and interface [7]. Considering interactions between all possible combinations of atoms and asuming that all species occupy the same area in the boundary, the Guttmann theory can be expressed in a generalized form for a multicomponent system by

$$\frac{X_I^{\phi}}{X^{0\phi} - \sum_J^{M-1} X_J^{\phi}} = \frac{X_I}{1 - \sum_J^{M-1} X_J} \exp\left(-\frac{\Delta G_I}{RT}\right) \tag{1}$$

where X_I^{ϕ} and X_I are the mole fractions of element I at the interface ϕ and in the bulk, respectively, and $X^{0\phi}$ is the total ratio of all sites available at the interface for segregation. The free energy of segregation, ΔG_I, is

$$\Delta G_I = \Delta H_I^0 - T\Delta S_I^0 - 2\alpha_{MI}\left(X_I^{\phi} - X_I\right) + \sum_{J\neq I}^{M-1} \alpha'_{IJ}\left(X_J^{\phi} - X_J\right) \tag{2}$$

[1] Structural defects can be classified according to their space dimensions as dimensionless (point) defects: vacancy, interstitial, quadruple grain boundary intersection junction; one-dimensional (line) defects: dislocation, disclination, triple grain boundary intersection line; two-dimensional (planar) defects: heterophase interface (liquid/gas, liquid/liquid, liquid/solid, solid/solid), homophase interface (grain boundary, stacking fault); three-dimensional (volume) defects: precipitates.

Table 1. The effect of individual variables on individual terms of Eq. (2).

Variable	ΔH_I^0	$T\Delta S_I^0$	$\alpha_{MI}\left(X_I^\phi - X_I\right)$	$\alpha'_{IJ}\left(X_J^\phi - X_J\right)$
System $M-I$	+	+	+	−
Additional solutes	−	−	+	+
Temperature	−	+	+	+
Type of interface	+	+	+	+
Orientation	+	+	+	+

where ΔH_I^0 and ΔS_I^0 are the standard molar enthalpy and entropy of segregation in a dilute binary $M-I$ system in which no interaction exists, and α_{MI} and α'_{IJ} are the parameters for binary interaction between atoms I in matrix M, and for ternary interaction between atoms I and J in the same matrix, respectively [7].

The complexity of equilibrium segregation to grain boundaries is displayed in Eq. (2). As shown in Table 1, the specific parameters of Eq. (2) depend on solute/matrix elements pairs, on the presence of additional solutes in the system and on their mutual interaction, on the temperature at which the segregation is equilibriated, on the type of the interface and on its crystallography [25]. Let us first briefly outline the effects of individual variables on equilibrium segregation.

2.1. *Binary Solute/Matrix Systems*

2.1.1. Langmuir-McLean Isotherm. An assumption of a binary $M-I$ system without interaction simplifies Eqs. (1) and (2) to the well-known form of the *Langmuir-McLean segregation equation* rewritten by Hondros and Seah [24] as

$$\frac{X_I^\phi}{X^{0\phi} - X_I^\phi} = \frac{X_I}{1 - X_I} \exp\left(-\frac{\Delta G_I}{RT}\right) \tag{3}$$

with

$$\Delta G_I = \Delta H_I^0 - T\Delta S_I^0 \tag{4}$$

This equation represents an analogy to the Langmuir gas adsorption isotherm and was originally derived by McLean [3] who used the statistical mechanics concept of the partition of solute atoms between two states of different free energy (bulk and interface). Equation (3) with condition (4) is the most frequently used segregation equation for binary systems. Because it ignores any interaction of solute atoms in the given matrix, the free energy of segregation, ΔG_I, is constant over the grain boundary and independent of the interface coverage below one monolayer. Therefore, it is only an approximation for real cases but it can be exactly veryfied for dilute systems with low grain boundary enrichment. Experimental verification of the validity of Eqs. (3) and (4) requires a precise quantitative measurement of the chemical composition of grain boundaries in the atomic monolayer region. Therefore, almost all data are obtained using surface analytical methods, in particular Auger electron spectroscopy (AES). In order to transform a grain boundary into a surface, *in situ* intergranular brittle fracture has to be carried out. All data referred to in this paper were obtained in this way.

The above mentioned conditions are attained in many systems, for example for S and In segregation in Ni, and for Si segregation in α-Fe. The values determined for the thermodynamic parameters ΔH_I^0 and ΔS_I^0 are listed in Table 2. In the Ni-S system, the average value $\Delta \bar{H}_S^0 = -70 \pm 10$ kJ/mol was found to fit best the temperature dependence of sulfur concentration at random grain boundaries of polycrystalline nickel [26]. On the other hand, segregation in both the other systems, Ni-In and Fe-Si, was measured at well-characterized interfaces. Indium segregation at {115} and {1 1 10} symmetrical tilt grain boundaries in a Ni-1.4 at.%In alloy can be correlated by approximately the same values of the segregation enthalpy, and the segregation entropy approaches zero at both boundaries [27, 28] (Fig. 1). A two times higher value of ΔH_{Si}^0

Table 2. Thermodynamic parameters of segregation in dilute binary systems which exhibit Langmuir-McLean behavior (Eqs. (3) and (4)).

Matrix	Segregant	Boundary	ΔH_I^0 (kJ/mol)	ΔS_I^0 (J/(mol.K))	Ref.
Ni	S	Polycrystal	−70		[26]
Ni-1.4 at.% In	In	150.6°[110], {115}	−38	0	[27, 28]
		163.5°[110], {1 1 10}	−39	0	[27, 28]
α-Fe-12.9 at.% Si	Si	70.5°[110], {112}	−4	−4	[29]
		36.9°[100], {013}	−8.1	−6.7	[29]

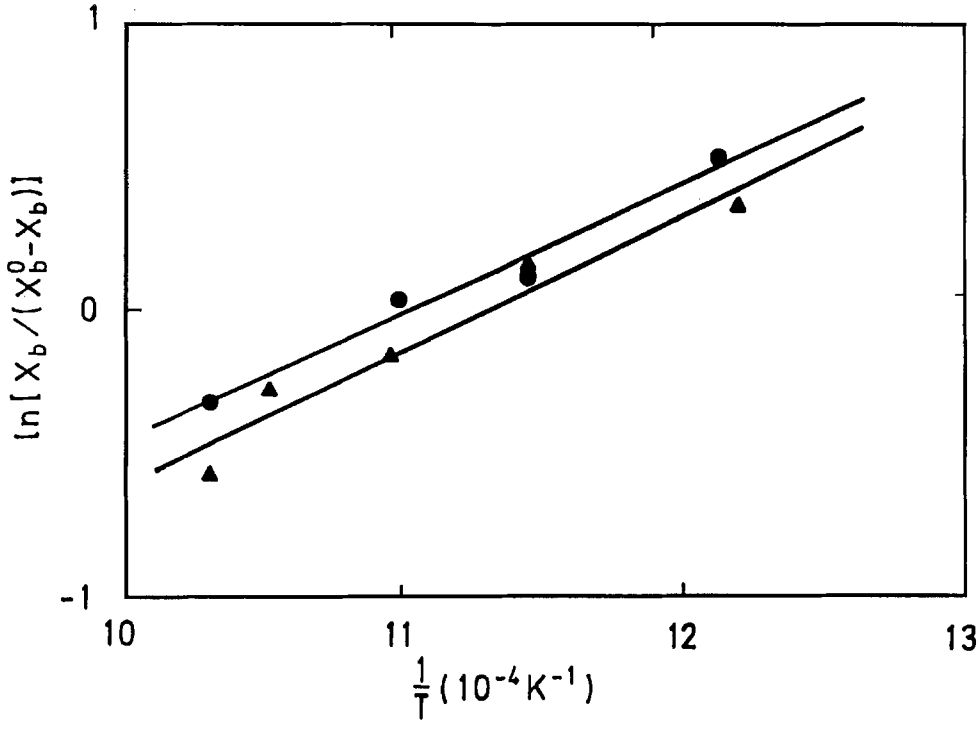

Figure 1. Arrhenius plot of the equilibrium segregation of In in Ni. Assuming $X^{0\phi} = 1$, X_{In}^{ϕ} was determined by Auger electron spectroscopy (AES) at two fracture surfaces of bicrystals with [110], {115} (•) and {1 1 10} (▲) symmetrical tilt grain boundaries. (After Muschik [27].)

was found for silicon segregation in an Fe-12.9 at.% Si alloy at the {013} as compared to the {112} symmetrical tilt grain boundary [29].

2.1.2. Prediction of Segregation in Binary Systems. Irrespective of the segregation measurement at random interfaces in polycrystals or at crystallographically well-characterized grain boundaries in bicrystals, pronounced differences in the values of ΔH_I^0 are apparent from Table 2 for individual systems. These differences can be well explained by the different solubility of individual solutes in the above mentioned matrix elements. Assuming a dilute alloy ($X_I \ll 1$) and introducing a bulk solid solubility limit X_I^* into Eq. (3), the expression

$$\frac{X_I^{\phi}}{X^{0\phi} - X_I^{\phi}} = \frac{X_I}{X_I^*} \exp\left(-\frac{\Delta G_I'}{RT}\right) \tag{5}$$

is obtained with

$$\Delta G_I' = \Delta G_I - \Delta G_I^{\text{sol}}. \tag{6}$$

Here, ΔG_I^{sol} is the free energy of solution of I in matrix M at the solid solubility limit ($X_I^* = \exp(\Delta G_I^{\text{sol}}/RT)$). Equation (5) is the so called *truncated BET isotherm* derived from the original BET (Brunauer-Emmett-Teller) multilayer gas adsorption equation by Hondros and Seah [24]. $\Delta G_I'$ is the difference of free energies of segregation and precipitation, and was empirically found to possess the value -10 ± 6 kJ/mol for all considered systems $M - I$ [30]. This allows to rewrite Eq. (5) into the form

$$\beta_I \equiv \frac{X_I^{\phi}}{X^{0\phi} X_I} = \frac{K}{X_I^*} \tag{7}$$

where β_I is the *grain boundary enrichment ratio* and $K = \exp(-\Delta G_I'/RT)$. Equation (7) represents a direct relationship between the grain boundary enrichment ratio and the solid solubility of a solute I in matrix M. Since

$$\Delta H_I^0 \propto RT \ln X_I^* \tag{8}$$

follows from combination of Eqs. (3), (4) and (7) for a dilute binary alloy assuming a negligible entropy term, the values of ΔH_I^0 as presented in Table 2 can directly be related to the logarithmic values of the corresponding bulk solid solubility: The value -70 kJ/mol was found for S segregation in Ni, in which the solubility of sulfur is a few ppm. With increasing solubility of

a solute in the matrix (e.g., 14 at% In in Ni or 30.5 at% Si in α-Fe), higher values of ΔH_I^0 were found (i.e., -38 or -39 kJ/mol for In in Ni, and -4 kJ/mol and -8.1 kJ/mol for Si in α-Fe). Recently, a detailed thermodynamic analysis [31] resulted in a more precise expression between the segregation enthalpy and bulk solid solubility, as discussed in more detail later in Section 2.6. Despite these refinements, Eq. (7) represents a direct relationship between the grain boundary enrichment ratio and the bulk solid solubility of a solute I in matrix M. Thus, Eq. (8) enables to predict the segregation tendencies in particular systems through knowledge of the bulk solid solubility.

2.1.3. Fowler Isotherm. In some systems, a strong interaction exists between solute atoms in a binary system $M-I$ so that the binary interaction term in Eq. (1) cannot be neglected. In this case, simplification of the general Eqs. (1) and (2) for a binary system leads to Eq. (3) with

$$\Delta G_I = \Delta G_I^0 - 2\alpha_{MI}\left(X_I^\phi - X_I\right) \qquad (9)$$

where $\Delta G_I^0 = \Delta H_I^0 - T\Delta S_I^0$. Assuming $X_I \ll X_I^\phi$ and $\alpha_{MI} = -Z_1\omega/X^{0\phi}$ where Z_1 is the lateral coordination number in the two-dimensional (2-D) segregation layer, and ω is the pair binding energy of segregant atoms I, the usual form of the *Fowler segregation isotherm* [32] is obtained. Of course, if no interaction exists, i.e., if $\alpha_{MI} = 0$, the ideal Langmuir-McLean segregation Eq. (3) with condition (4) is obtained. The case $\alpha_{MI} > 0$, i.e., $\omega < 0$ means attractive interaction and increases the apparent free energy of segregation with the segregation level X_I^ϕ according to Eq. (9). The Fowler behavior was observed for Te and Se segregation in α-Fe [33] and for Bi segregation in Cu [34]. For strong interactions, e.g., for $\alpha_{MI}X^{0\phi} = 6RT$, a condensation of a 2-D phase can be expected. Such a 2-D structure was found for Nb segregation at stacking faults in a Co-0.96 at.% Nb alloy [35].

2.2. *Presence of Additional Solutes: Multicomponent Systems*

Segregation in multicomponent systems with two or more solutes often results in a rather complex segregation behavior depending on the type and magnitude of solute interaction. In general, segregation in a multicomponent system can be described by Eq. (1) with condition (2). However, as shown by Guttmann and McLean [7] and discussed by Militzer and Wieting [36], some modifications of these equations can arise for cases in which segregation of different solutes occurs at different grain boundary sites, e.g., if substitutional and interstitial sites are distinguished, and with or without considering site competition of solute atoms at the boundary.

2.2.1. Site Competition. Even in the case when no interaction occurs in a multicomponent alloy, site competition can affect the segregation behavior of individual solutes. This site competition is involved in the denominator of the ratio at the left-hand side of Eq. (1) and shows how the solutes compete for the totally available sites $X^{0\phi}$: Segregation of a solute I is reduced by those of other solutes and vice versa. As a result, a strong segregant can completely expel a weaker segregating solute (lower $|\Delta G_I|$) from the interface especially at low temperatures. Site competition at grain boundaries was observed e.g., for C and P, and O and P in W containing additions of Fe and Ni (Fig. 2) [37].

2.2.2. Mutual Interaction. In contrast to site competition influencing segregation levels through the changes of interfacial concentration of additional solutes, mutual interactions of solute atoms affect grain boundary segregation through changes of the apparent segregation free energy according to Eq. (2). These interactions can be either attractive as characterized by negative values of corresponding α'_{IJ}, or repulsive with $\alpha'_{IJ} > 0$. Attractive interactions lower the apparent (negative) free energy of segregation of both interacting solutes and thus lead to synergetic cosegregation of these solutes. Strong interaction with a low value of α'_{IJ} can result in the formation of 2-D interfacial compounds of the interacting elements [7]. On the other hand, repulsive interaction increases the value of ΔG_I and, therefore, suppresses the segregation of the two solutes. The final result of repulsive interactions is similar to that of site competition and sometimes it is difficult to distinguish between them. However, the basic mechanisms are different as described above.

There are many systems in which solute interactions play a substantial role in segregation behavior as pointed out by Guttmann and McLean [7]. Hofmann and Hofmann [37] observed attractive interaction between Ni and P atoms, and between Fe and P atoms in a tungsten matrix (Fig. 2) and Otterbein [38] found attractive interaction between Ni and B atoms in Ni-rich Ni_3Al intermetallics ($\alpha'_{NiB} = -34$ kJ/mol). On the

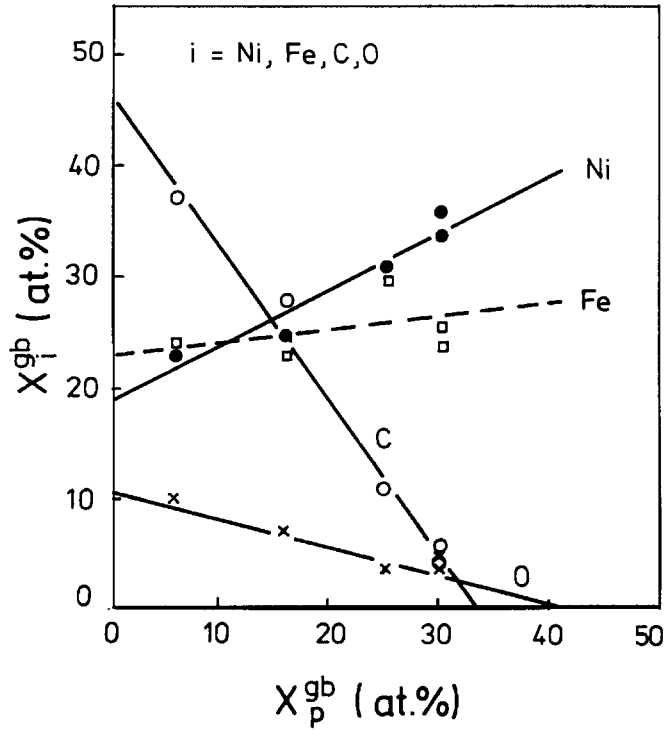

Figure 2. Correlation between the grain boundary concentration of P (X_P^{gb}) and that of Ni, Fe (cosegregation) and C, O (site competition) at intergranular fracture surfaces of a W base alloy studied by Auger electron spectroscopy. (After Hofmann and Hofmann [37].)

other hand, Lejček and Hofmann [39] observed strong repulsive interaction between Si and P atoms in a P-doped Fe-Si alloy ($\alpha'_{SiP} = 92$ kJ/mol).

2.2.3. Activity Approach. Starting with the discussion of cosegregation of Ni and Sb in Fe base alloys described by Gas et al. [40], Briant [41] gave rise to doubts about the concept of atomic interaction in multicomponent alloys and later proposed to explain the changes of segregation behavior caused by the presence of additional solutes in a system—beside site competition—by changes in bulk activities of individual solutes and by mutual changes of their solubilities [42]. Then, the concept of chemical equilibrium thermodynamics can be adapted for description of interfacial segregation

$$\frac{a_I^\phi a_J}{a_J^\phi a_I} = K_r \qquad (10)$$

where a_i is the activity of a solute i ($i = I, J$) in a ternary $M - I - J$ system at an interface ϕ and in bulk. $K_r = \exp(-\Delta G_r/RT)$ is a constant of a "reaction"

$$I + J^\phi \rightleftharpoons I^\phi + J \qquad (11)$$

and ΔG_r is the standard molar free energy of reaction (11). The reaction constant K_r is only temperature dependent.

This concept does not seem to be more useful than the original Guttmann theory. First, the value of ΔG_r is related to segregation of a given pair of solutes according to Eqs. (10) and (11), and does not characterize the segregation tendency of a single solute in a given matrix (in fact, ΔG_r is the difference of ΔG_i for individual segregants I and J). Second, the handling with activities in Eq. (10) is more complicated than with concentrations in Eq. (1). Strictly speaking, the effect of changed activities by addition of the additional element [42] can be approached more transparently by considering the interaction approximation [7]. Despite of the formal differences in the description of individual models [7, 42], a recent observation of segregated surfaces of a P-doped Fe-Si alloy by scanning tunelling microscopy revealed the existence of islands of segregated phosphorus at the surface, the vicinity of which was completely free of silicon [43]. This demonstrates that a rather repulsive interaction exists between P and Si atoms (at least at the surface) instead of only a simple site competition.

2.2.4. Segregation Enthalpy. The Guttmann model was successfully applied to explain our measurements in several multicomponent systems. Besides for the polycrystalline Fe- and Ni-doped W base alloy [37] already mentioned above, Eqs. (1) and (2) have been used to correlate the temperature dependences of grain boundary composition of well-characterized grain boundaries in an Fe-3.55 at.% Si alloy [39, 44–47], and in a Ni-rich $Ni_3Al(B)$ [38]. The respective values of segregation enthalpies ΔH_I^0 and entropies ΔS_I^0 determined in these studies at individual grain boundaries are compiled in Table 3.

Let us now compare the values of ΔH_{Si}^0 determined for the {112} and {013} grain boundaries in different Fe-Si alloys. While the values for a binary Fe-12.9 at.% Si alloy were determined according to the Langmuir-McLean model (Table 2), the values for a multicomponent Fe-3.55 at.% Si alloy were obtained from the correlation to the Guttmann model (Table 3). It is seen that the corresponding values of ΔH_{Si}^0 are very similar. In addition, excellent agreement was found between the values of ΔH_{Si}^0 and ΔH_P^0 determined experimentally for the {013} grain boundary (Table 3) with the values of the segregation energy, $E_{Si}^{seg} = -9.8$ kJ/mol, and $E_P^{seg} = -14.6$ kJ/mol calculated for the same boundary by Masuda-Jindo [48]. All these findings support the assumption that the quantity ΔH_I^0 is independent of the alloy composition and thus, it is representative for the segregation of solute I in the pure matrix M.

2.2.5. Segregation Entropy. A similar conclusion cannot be drawn for the quantity ΔS_I^0. Although the differences between ΔS_{Si}^0 determined for the Fe base alloys containing 12.9 at.% Si (Table 2) and 3.55 at.% Si (Table 3) are not large, very high values of ΔS_P^0 were found for phosphorus segregation, mainly at low-index grain boundaries in the latter alloy. An analysis of Seah and Lea [49] disclosed that ΔS_I^0 generally consists of three terms which are associated with changes in the vibrational, anharmonic and site multiplicity contributions. An estimate of these contributions suggests that the absolute value of the entropy of grain boundary segregation should be lower than $3.3R$, i.e., 27.4 J/(mol.K). In addition to our values listed in Table 3, however, the values of the segregation entropy exceeding this limit were found experimentally in α-Fe base alloys in other studies ($\Delta S_{Sn}^0 \approx 5.4R$ for $T \leq 1184$ K and $\Delta S_{Sn}^0 \approx 6.4R$ for $T \geq 1184$ K [49] or $\Delta S_C^0 \approx 5.2R$ [50]). This disagreement of the experimental data with the prediction is not completely clear till now. We can well assume that the mutual interaction of segregants in a multicomponent alloy not only affects the segregation enthalpy but also the segregation entropy and thus, ΔS_I^0 does not characterize solute segregation of a solute I in a pure matrix M as does ΔH_I^0.

2.2.6. Thermodynamics of Segregation in Polycrystals. It is apparent from Table 3 (and will be thoroughly discussed in Section 2.4.) that individual grain boundaries in a given matrix often possess very different values of ΔH_I^0 and ΔS_I^0. However, segregation is frequently measured at numerous crystallographically non-specified grain boundaries in polycrystals. In this case the mean values of $\Delta \bar{H}_I^0$ and $\Delta \bar{S}_I^0$ are usually evaluated according to an appropriate segregation isotherm from the temperature dependence of arithmetical averages of chemical composition for individual polycrystalline specimens (e.g., [51]). The use of maximum values of grain boundary segregation at individual temperatures (that seem to correspond to the same type of grain boundaries) was proposed as another alternative for evaluation of the thermodynamic parameters [52]. Thus, the question arises about the physical meaning of the quantities $\Delta \bar{H}_I^0$ and $\Delta \bar{S}_I^0$ determined in this way. In order to find a relationship between $\Delta \bar{H}_I^0$ and $\Delta \bar{S}_I^0$, and the corresponding values of segregation enthalpies and entropies, respectively, for individual grain boundaries, Lejček [53] modeled polycrystalline fracture surfaces from the boundaries of known segregation behavior and found that this relationship is very complex. Only if the arithmetic average of the boundary concentration is equal (or close) to the geometric average, the values of $\Delta \bar{H}_I^0$ and $\Delta \bar{S}_I^0$ represent the arithmetic averages of ΔH_I^0 and ΔS_I^0 of individual grain boundaries. The value $\Delta \bar{H}_P^0 = -33$ kJ/mol determined from these model calculations is in very good agreement with the value -34.3 kJ/mol found by Erhart and Grabke [51] for phosphorus segregation in polycrystalline α-Fe. The use of maximum values of grain boundary segregation for determination of "more realistic" values of parameters $\Delta \bar{H}_I^0$ and $\Delta \bar{S}_I^0$ was found to be very sensitive to the random presence of a single grain boundary exhibiting large segregation effects at the fracture surface [53]. Another reasonable description of grain boundary segregation in polycrystals seems to be the use of a spectrum of grain boundary free energies [54–56].

Table 3. Thermodynamic parameters of segregation in ternary systems calculated according to the Guttmann segregation isotherms (Eqs. (1) and (2)).

Matrix	Segregant	Boundary	ΔH_I^0 (kJ/mol)	ΔS_I^0 (J/(mol.K))	Ref.
α-Fe-3.55at.% Si	Si	70.5°[110], {112}	−3	−3.8	[39]
	P		−7.9	+42.7	[39]
	Si	18.9°[100], {016}	−16	−15	[47]
	P		−31	+17	[47]
	C		−49	+1	[47]
	Si	22.6°[100], {015}	−12	−9	[46]
	P		−16	+38	[46]
	C		−43	+7	[46]
	Si	28.1°[100], {014}	−14	−9	[46]
	P		−35	+19	[46]
	C		−50	+2	[46]
	Si	36.9°[100], {013}	−8.5	−3	[44]
	P		−13.3	+45.2	[44]
	C		−40	+12	[44]
	Si	36.9°[100], (018)/(04$\bar{7}$)	−10	−8	[45]
	P		−32	+19	[45]
	C		−50	+3	[45]
	Si	36.9°[100], (001)/(03$\bar{4}$)	−9	−3	[45]
	P		−25	+29	[45]
	C		−44	+6	[45]
	Si	36.9°[100], (0$\bar{1}$7)/(01$\bar{1}$)	−6.1	−2.2	[45]
	P		−14.5	+39.3	[45]
	C		−36	+14	[45]
	Si	36.9°[100], (0 $\bar{3}$ 11)/(09$\bar{7}$)	11	−5	[45]
	P		−32	+21	[45]
	C		−48	+3	[45]
	Si	45.2°[100], {0 5 12}	−17	−13	[46]
	P		−37	+18	[46]
	C		−51	+6	[46]
	Si	50.0°[100], {0 7 15}	−12	−3	[46]
	P		−31	+25	[46]
	C		−45	+6	[46]
	Si	53.1°[100], {012}	−4.1	+0.2	[44]
	P		−10.9	+42.5	[44]
	C		−35	+12	[44]
	Si	58.1°[100], {059}	−12	−5	[46]
	P		−34	+20	[46]
	C		−48	+4	[46]
	Si	64.0°[100], {058}	−16	−11	[46]
	P		−37	+16	[46]
	C		−53	−1	[46]
Ni-rich Ni_3Al	Ni	50.5°[110], {113}	−39	−25	[38]

The above discussion about the character of segregation entropy and Briant's proposals of an alternative description of grain boundary segregation suggest that the present phenomenological theories—although well elaborated—are based on a number of simplifications which may not be fulfilled in reality [57]. In addition, the total number of available segregation sites may change due to segregation or due to transformation of the grain boundary structure resulting from the segregation similarly to those described recently by Paidar et al. [58]. Phenomenological theories, indeed, do not provide numerical values for segregation and for interaction parameters. A detailed description of a segregation system including prediction of these parameters should be based on atomistic aspects of bonding including structural factors [2].

2.3. *Segregation Temperature*

As predicted theoretically and observed experimentally, solute segregation at an interface decreases with increasing temperature in a binary alloy [4, 10]. This is also apparent from Fig. 1. However, in a multicomponent system, segregation behavior can be modified due to site competition and mutual interaction of individual pairs of solutes. This can be documented for an example of phosphorus, silicon and carbon segregation at grain boundaries of iron (Fig. 3). Since interaction between carbon and both other solutes is practically negligible [44] and the total amount of segregation is low, no site competition occurs, and thus carbon segregates independently of the presence of other solutes. On the other hand, there is a very large repulsive interaction between phosphorus and silicon (92 kJ/mol) [39]. Due to this repulsion, more surface active phosphorus segregates at grain boundaries in the temperature range 773 K–1173 K and repels silicon to such an extent that its depletion occurs. With increasing temperature the amount of segregating phosphorus decreases and silicon is allowed to segregate in larger extent. Therefore, apparently reversed temperature dependence of silicon segregation occurs as a result of this interaction. Nevertheless, considering mutual interaction, negative values of segregation enthalpies are obtained also for silicon segregation (cf. Table 3).

A detailed analysis of temperature dependence of grain boundary segregation at individual grain boundaries in a multicomponent system containing a trace impurity characterized by high tendency to segregation (high $|\Delta H_I^0|$) and a solute with a low tendency to segregation (low $|\Delta H_J^0|$) in concentrations of the order of units of atomic percent was made in paper [59]. This analysis shows a basic property of this system: At low temperatures the impurity segregates strongly so that its concentration at the boundary reaches almost saturation whereas the solute is not present at the boundary. With increasing temperature the grain boundary concentration of the impurity decreases slowly and allows the solute to segregate. This course is characteristic for segregation behavior of multicomponent systems with site competition of segregants. If in addition repulsive interaction exists, the segregation of the solute with low $|\Delta H_J^0|$ is more suppressed and the transition region (i.e., decrease of impurity segregation and increase of solute segregation) is shifted to higher temperatures. Similarly, the lines of temperature dependence of solute segregation are shifted for grain boundaries possessing different values of segregation enthalpy (and entropy) for elements involved. Because the temperature dependence of grain boundary segregation of a solute with low $|\Delta H_I^0|$ is S-shaped with $X_J^\phi \to 0$ for low temperatures, a temperature region must always exist in which a depletion of grain boundaries by atoms of this solute is observed. It is clear from the above discussion that a temperature will exist for different sets of ΔH_I^0 and ΔS_I^0, at which the solute will enrich one boundary while its depletion will be observed at another one. This "qualitative" difference was observed for silicon segregation at the {112} and {013} symmetrical tilt grain boundaries in an Fe-Si-P-C multicomponent system [39, 44].

2.4. *Grain Boundary Orientation: Anisotropy of Segregation*

A grain boundary in a solid possesses the atomic structure resulting from a particular combination of five main variables (degrees of freedom), i.e., rotation axis, misorientation angle and grain boundary plane normal. The fact that it is controlled by five parameters suggests that there is a huge number of grain boundaries which may differ in their properties. In principle, however, we can distinguish between two main groups of interfaces which fundamentally differ in their structures and thus in their segregation behavior: a few *special* grain boundaries with the structure formed by single structural units, and a majority of *general* grain boundaries, which are composed of combinations of structural units of the special ones [60]. Although the

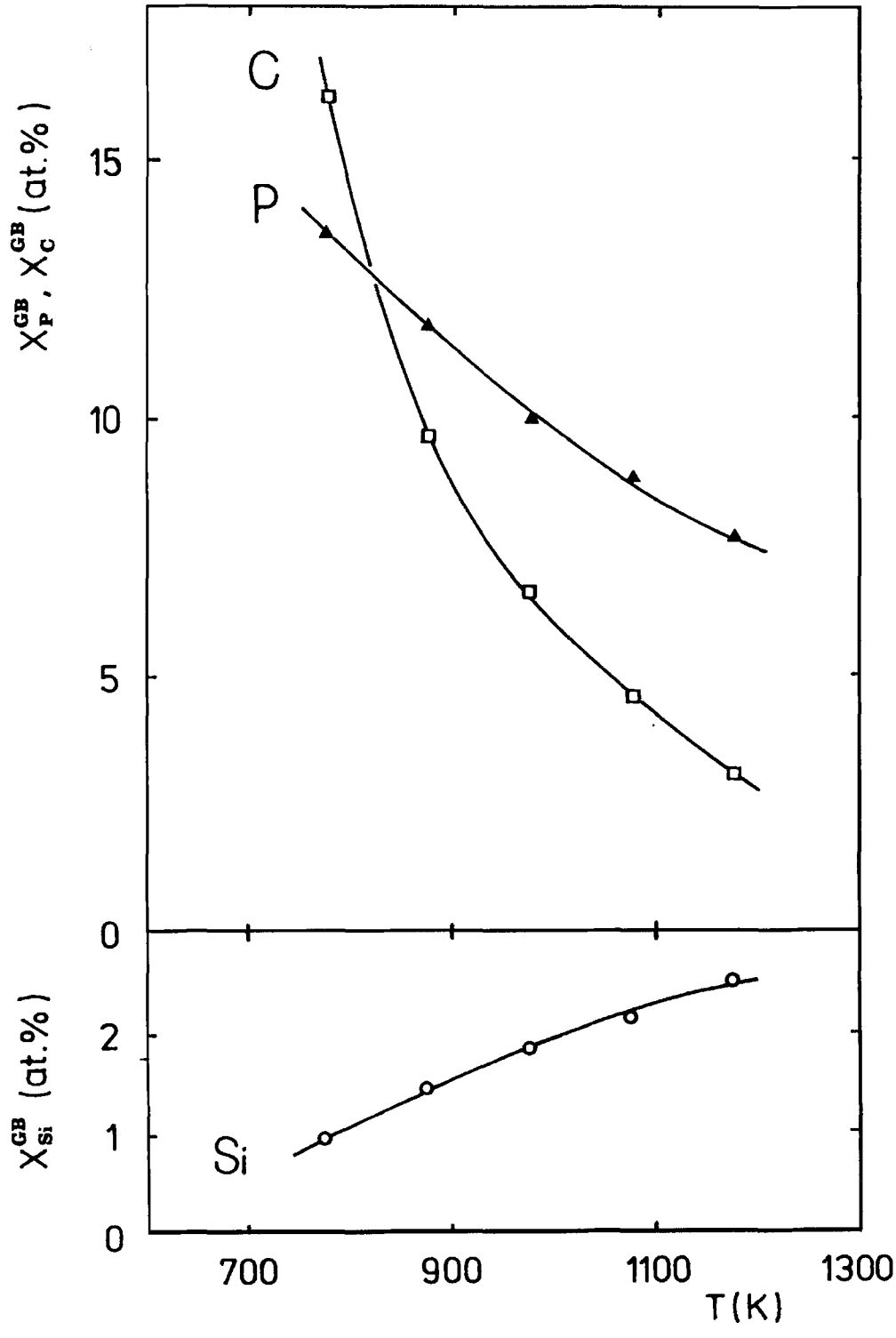

Figure 3. Temperature dependence of C, P and Si segregation at the {013} symmetrical grain boundary studied by Auger electron spectroscopy. (After Lejček and Hofmann [44].)

number of the fundamental structural units is limited, the transition between these two groups of grain boundaries is still not clear, and further special boundaries are experimentally identified. Current effort is therefore focussed on searching for these interfaces and for a simple (geometric) criterion for special grain boundaries [2].

2.4.1. Orientation Dependence of Grain Boundary Concentration. It is obvious that grain boundary segregation increases with increasing misorientation angle of the two adjoining grains from $\theta = 0$ (no boundary, single crystal) to $\theta = 10 \cdots 15°$ [61–65]. This increase is closely connected with densifying array of dislocations forming their structures. In some cases such as Si segregation in Fe [66], no apparent segregation of a weak segregant is observed. After the change of the grain boundary structure from the dislocation one to that formed by structural units, an abrupt change of the orientation dependence of grain boundary segregation can be observed [61]. Generally, these changes are more pronounced for tilt than for twist grain boundaries due to the different ability of edge and screw dislocations to accomodate foreign atoms [67].

Measurements of solute segregation at high angle grain boundaries ($\theta > 15°$) have been performed more frequently than at low angle ones. The results sometimes appear to be contradictory, thus revealing the complexity of the structural dependence of grain boundary segregation. If grain boundary concentrations or its representative (e.g., relative Auger peak-to-peak heights) are plotted against the total misorientation angle without keeping the other degrees of freedom constant, largely scattered data are usually obtained and permit to conclude only qualitatively that solute segregation monotonously increases with increasing θ [52, 62, 65, 66]. However, the character of a plot of the data corresponding to a single rotation axis and to symmetrical tilt grain boundaries can be markedly different: Low segregation is usually detected at certain (special) grain boundaries as compared to very similar high levels of segregation at the other (general) ones [63, 64]. In some cases, other types of such non-monotonous orientation dependences were reported, as e.g., a broad minimum of Bi segregation at [100] grain boundaries in Cu over a range of orientations [68] or maxima of grain boundary segregation for Si in a 17Cr–13Ni stainless steel at grain boundaries which are considered as special [69]. In the case of twist grain boundaries, the orientation dependence is expected to be less pronounced as at the tilt ones, but even in this case, a pronounced cusp was found for Re segregation at the 70.5°(110) twist grain boundary in tungsten while the general tendency of Re segregation is to increase with increasing rotation angle [70, 71]. Surprisingly, higher Si segregation was recently detected at the twist grain boundaries in iron as compared to tilt interfaces by Krakauer and Seidman [72]. In the case of asymmetrical grain boundaries the grain boundary plane orientation strongly affects segregation levels. Suzuki et al. [73] found large phosphorus segregation at grain boundary planes characterized by high values of Miller indices whereas low segregation was observed at low-index grain boundary planes despite of the orientation of the other boundary plane. Similarly, no sulfur segregation was detected at coherent twin boundaries and at symmetrical {113} grain boundary in nickel whereas a sulfur enrichment was observed at many asymmetrical grain boundaries possessing relatively high Miller indices [74, 75].

Grain boundary concentration of an element in a given matrix depends on both the temperature and on presence of other solutes or impurities there. Therefore, an orientation dependence of chemical composition of a grain boundary can well represent the anisotropy of grain boundary segregation only in the case of dilute binary systems equilibriated at the same temperature. In a multicomponent system, however, such a plot can be misleading. This is apparent, for example, from the measurements of grain boundary segregation in an Fe-3.55 at.% Si alloy containing traces of phosphorus and carbon [46]. As it is seen from Fig. 4, the orientation dependence of carbon concentration at grain boundaries exhibits minima for the 53.1°[100], {012}, 36.9°[100], {013} and 22.6°[100], {015} grain boundaries. In the case of phosphorus and silicon, the orientation dependences are less clear. Minima of phosphorus segregation can be recognized at {012} and {015} grain boundaries at 773 K. However, we can find three maxima at {012}, {013} and {015} grain boundaries at 1173 K. The orientation dependence of silicon segregation is much more complicated. A depletion of Si occurs at particular grain boundaries at low temperatures and a non-monotonous increase of its grain boundary concentration occurs with increasing temperature. This complex segregation behavior of individual grain boundaries is a consequence of the important role of site competition and mutual interaction in a multicomponent system [59] as was already discussed in

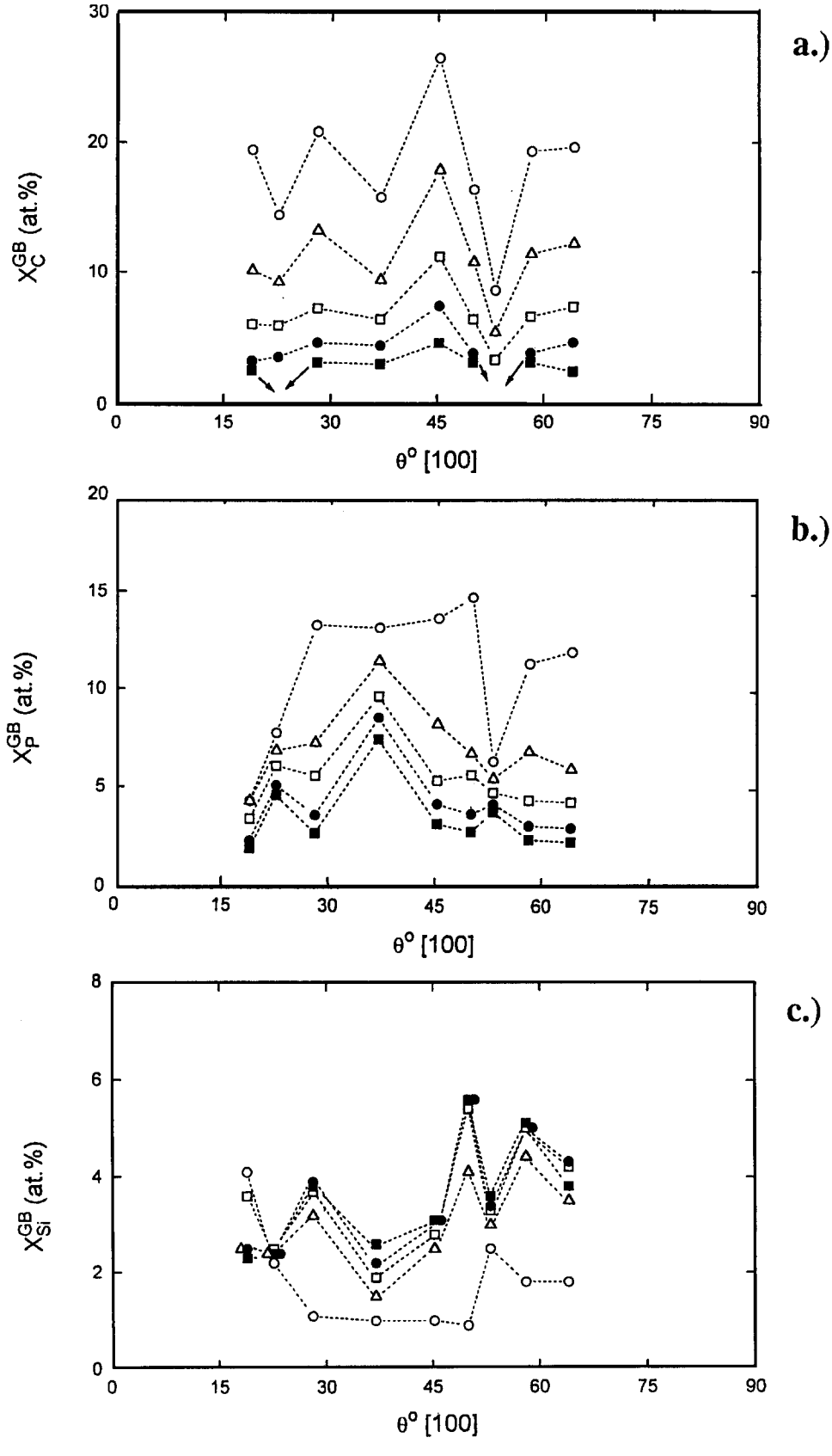

Figure 4. Orientation dependence of (a) carbon, (b) phosphorus, and (c) silicon segregation at symmetrical tilt grain boundaries of an Fe-Si-P-C system at 1173 K (○), 1073 K (△), 973 K (□), 873 K (●) and 773 K (■). (After Hofmann et al. [46].)

Part 2.3. The character of the orientation dependence of phosphorus segregation (Fig. 4) is qualitatively similar to that of silicon segregation in a Cr-Ni stainless steel [69]. This comparison suggests that the reported grain boundary segregation of silicon in this stainless steel [69] should be affected by the interaction of silicon with an additionally present alloying or impurity element.

2.4.2. Orientation Dependence of Segregation Enthalpy. As proposed above, an independent thermodynamic state quantity such as a standard molar segregation enthalpy ΔH_I^0 of a particular binary system can be used to represent the segregation tendency of an element in such systems (cf., Eq. (2) and Table 1). As it is apparent from Table 3, we determined this quantity for many well-characterized grain boundaries in bicrystals of several alloys that enables us to compare the segregation tendencies of individual grain boundaries for various binary systems. Relatively low values of $\Delta H_{\text{In}}^0 = -38$ and -39 kJ/mol for In segregation at {115} and {1 1 10} grain boundaries of Ni together with a negligible segregation entropy of both these interfaces result in the value -34 kJ/mol for the free energy of segregation of these boundaries at 970 K. This value, which is substantially higher than $\Delta G_{\text{In}}^0 = -50$ kJ/mol found for polycrystals suggests a rather low segregation tendency of these [110] grain boundaries [27, 28]. An estimate of segregation free energies of boron and nickel in Ni-rich Ni_3Al suggests very low tendency of both elements to segregate at the $\Sigma = 3$, {111} and $\Sigma = 11$, {113} symmetrical tilt grain boundaries as compared to the other symmetrical grain boundaries corresponding to the same values of Σ, {112} and {233}, respectively [38].

The orientation dependences of ΔH_I^0 for the Si, P and C segregation at various [100] tilt grain boundaries of α-Fe are shown in Figs. 5 and 6. In contrast to grain boundary composition (Fig. 4), the orientation dependences of $-\Delta H_I^0$ for all three elements are qualitatively similar and exhibit pronounced cusps at the 22.6°[100], {015}, 36.9°[100], {013} and 53.1°[100], {012} tilt grain boundaries [46, 47]. Qualitatively similar dependences of segregation enthalpies for the same elements were found for 36.9°[100] asymmetrical tilt grain boundaries. In this case, the cusps are located not only at the two symmetrical tilt grain boundaries characterized by the deviations $\psi = 0°$ and $\psi = 45°$ from the symmetrical {013} grain boundary, but also at the $\psi = 18.4°$, $(001)/(03\bar{4})$ and $\psi = 26.6°$, $(0\bar{1}7)/(01\bar{1})$ asymmetrical ones [45]. The

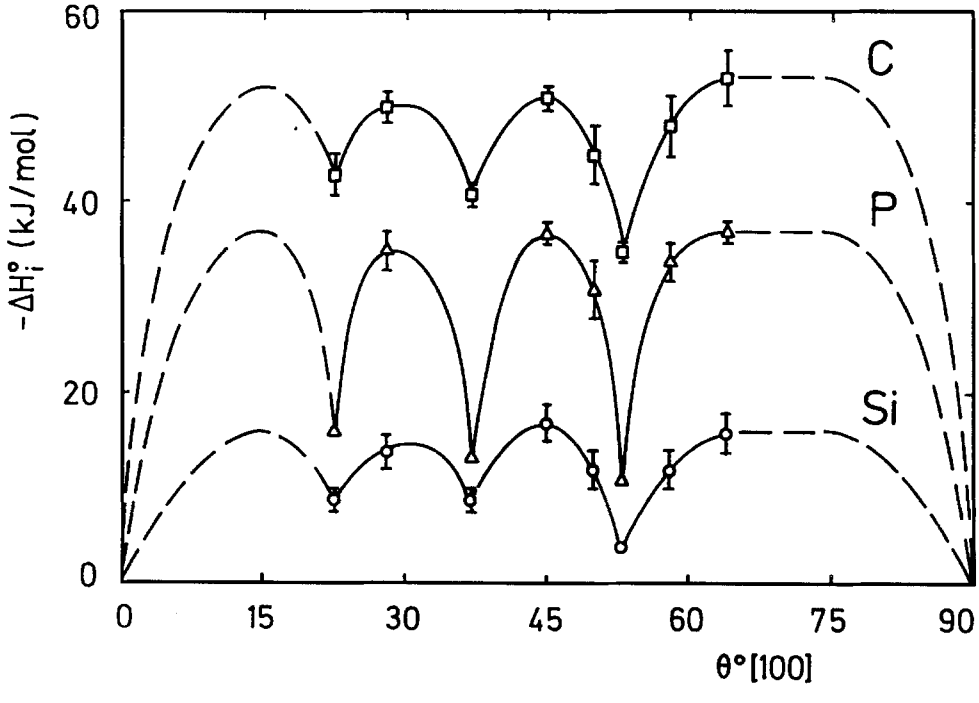

Figure 5. Dependence of segregation enthalpies ΔH_I^0 (I = C, P, Si) on the misorientation angle θ of both adjacent grains in [100] symmetrical tilt bicrystals of an Fe-3.55at.%Si alloy. (After Hofmann et al. [46].)

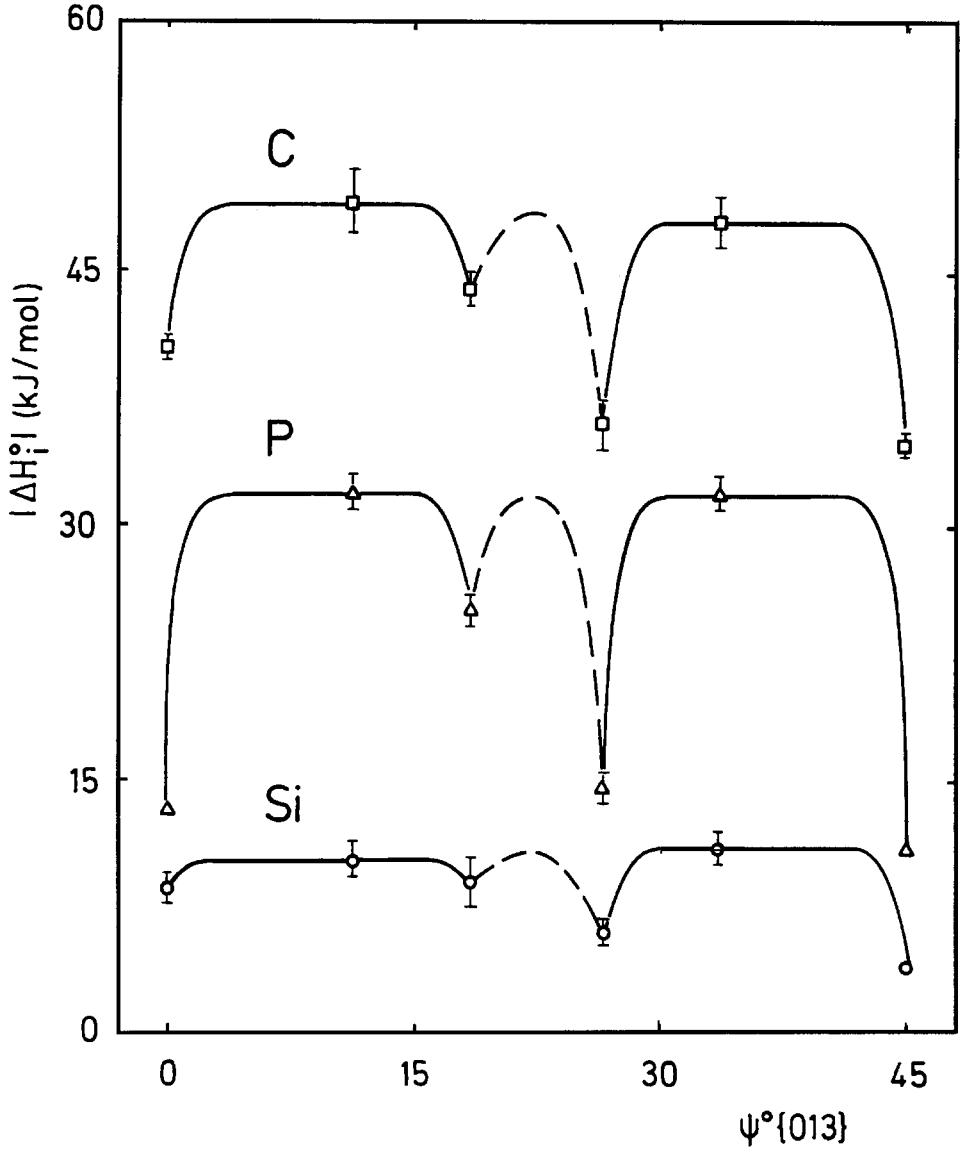

Figure 6. Dependence of segregation enthalpies ΔH_I^0 (I = C, P, Si) on the deviation angle ψ of the boundary plane from the {013} symmetrical grain boundary in the 36.9°[100] tilt bicrystals of an Fe-3.55 at.% Si alloy. (After Lejček et al. [45].)

values of segregation enthalpies of particular elements at individual grain boundaries were correlated to some geometrical factors, for example to the reciprocal density of the coincidence site lattice, Σ, and to the effective interplanar spacing, d_{eff}/a, related to the lattice parameter a, as introduced by Wolf [76]. This correlation clearly showed that the parameter d_{eff}/a is very useful for characterization of special tilt grain boundaries [2, 77, 78]. This is because the interplanar spacing is in a close relationship to the hierarchy of geometric classification of tilt grain boundaries based on the creation of their structural units [79, 80]. The parameter Σ can be well correlated with the behavior of symmetrical grain boundaries (i.e., special boundaries possess low values of Σ), however, it fails if asymmetrical grain boundaries are considered which belong to the same Σ but which can differ in their behavior [2]. In addition, some asymmetrical grain boundaries such as 45°[100], (001)/(011) having incommensurate structures with $\Sigma \to \infty$, were found to be special. For illustration, the dependence of $-\Delta H_I^0$ on the effective interplanar spacing is shown in Fig. 7 [2].

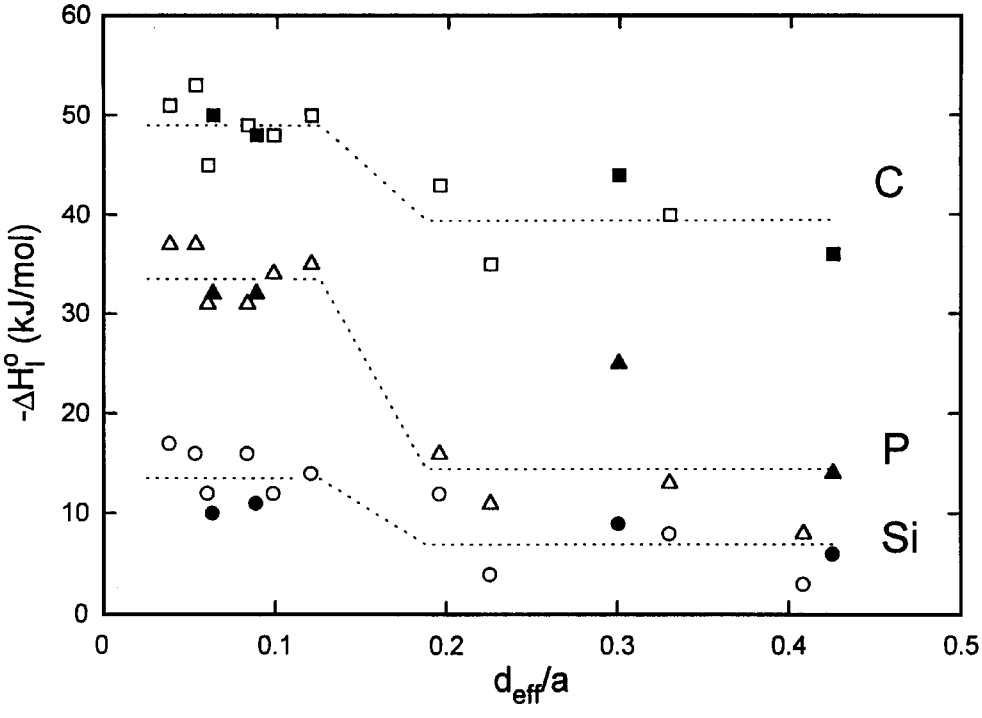

Figure 7. Plot of segregation enthalpies ΔH_I^0 of carbon (□), phosphorus (△) and silicon (○) in α-Fe vs. interplanar spacing, d_{eff}/a for some symmetrical (open symbols) and asymmetrical (solid symbols) tilt grain boundaries. (After Lejček and Hofmann [2].)

2.5. *Type of the Interface: Grain Boundary vs. Surface Segregation*

As discussed at the beginning of Chapter 2, the nature of solute segregation is the same for all structural defects and, in principle, can be described by the same type of the segregation equation as e.g., Eqs. (1) and (2). Since the average free energy of general grain boundaries in metals is about $1/3 - 1/2$ of that of free surfaces, the free energy of grain boundary segregation will generally be lower than that of free surfaces [15]. Therefore, technically easier experiments on surface segregation have often been used to estimate the character and amount of interfacial segregation, for example [81–83]. This qualitative estimate can be well made, however, only in binary alloys whereas it can fail in complex multicomponent systems since the presence of an additional element can induce significant differences between segregation behaviors of grain boundaries and free surfaces as a result of changing effect of mutual interaction of individual solutes and their site competition [84].

Different segregation behavior in ternary or multicomponent systems can be well documented by simultaneous study of grain boundary and free surface segregation in the same sample. A novel technique to measure the temperature dependences of surface and grain boundary segregation was developed by Muschik et al. [85] for oriented bicrystals prepared by diffusion bonding. In this technique two single crystals were mutually suitable oriented and bonded to obtain a bicrystal with the boundary of desired orientation. Before this procedure, however, the surface of one of these crystals was etched in a periodic pattern of circular cavities having diameter of 100 μm and depth of several μm. Thus, both the grain boundary and the free surface were present in the same sample and were thermally treated in the same way. After fracture *in situ* in the AES analysis chamber, both the artificial cavities, i.e., the free surface, and the fractured grain boundary could be analyzed. The study of solute segregation at both the grain boundaries and the free surfaces in a Ni-In alloy revealed that In segregation dominates at grain boundaries accompanied by weak segregation of sulfur, whereas extensive segregation of sulfur suppresses In segregation at free surfaces of the same crystallography [86] (Fig. 8). Similarly, an extensive S segregation and only slight enrichments of B and Ni were observed

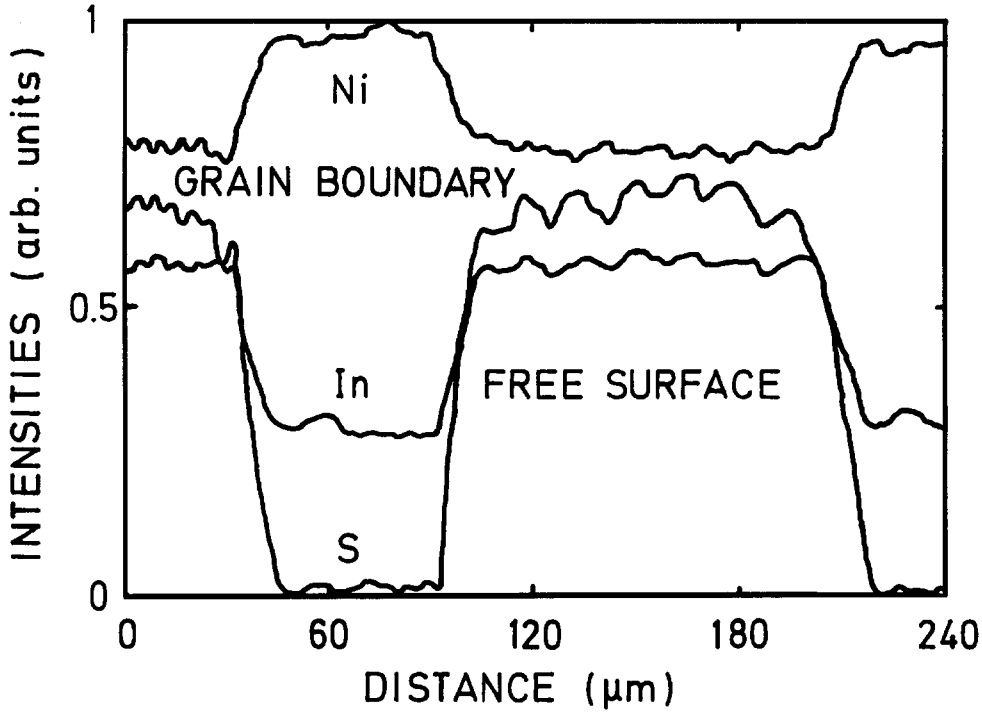

Figure 8. Elemental line scan obtained by Scanning Auger Microscopy at the fracture surface of a bicrystal of an Ni-1.4 at.% In alloy with traces of S containing the {115} grain boundary with artificial cavities showing different segregation behavior of In and S at free surface (i.e., cavities) and grain boundaries (i.e., fracture surface). (After Muschik et al., [85].)

at free surfaces of a Ni-rich Ni_3Al alloy. On the other hand, both B and Ni segregate at the grain boundaries where the enrichment of sulfur was negligible [38, 87].

Qualitative differences in the segregation behavior of surfaces and grain boundaries can occur in systems with strong attractive interaction of two segregants resulting in the formation of 2-D surface compounds. This type of the behavior was observed in an Fe-Si base alloy. As described in Section 2.3, an enrichment of carbon and phosphorus and a depletion of silicon characterize the segregation behavior at the {013} symmetrical tilt grain boundary at 873 K while nitrogen is practically not detected there [44, 88]. Annealing of the sputtered fracture surface from this boundary, i.e., now a (013) free surface, at the same temperature, however, leads to formation of stable Si_xN_y 2-D surface compounds at this surface thus preventing segregation of other elements. In denitridized and decarburized samples, on the other hand, enrichment of phosphorus and depletion of silicon were found again at the grain boundary whereas pronounced sulfur segregation dominates at the free surface and is accompanied by a weaker phosphorus and silicon segregation [88, 89]. Model calculation of the segregation behavior in an Fe-Si (P, S) alloy demonstrated that the differences in the behavior of both crystallographic interfaces are controlled by the free energy of segregation of individual components. This calculations disclosed that sulfur does not segregate at grain boundaries in a detectable amount even at very low bulk concentrations of phosphorus. On the other hand, sulfur segregation dominates at the (013) surface and starts to be replaced by phosphorus segregation only at relatively high bulk amounts of phosphorus ($X_P > 10X_S$) (Fig. 9). From the phenomenological point of view these qualitative differences may be considered as a *generalized anisotropy of interfacial segregation* [88, 89].

2.6. *Predictive Capabilities: Grain Boundary Segregation Diagrams*

As mentioned in Section 2.1.2., Seah and Hondros [30] suggested a method for an order-of-magnitude prediction of grain boundary composition from the knowledge of the bulk solid solubility of a solute in a given matrix. The qualitative similarity of orientation dependences of grain boundary segregation in Fe-Si and Fe-Sn systems allowed Watanabe et al. [62] to extend

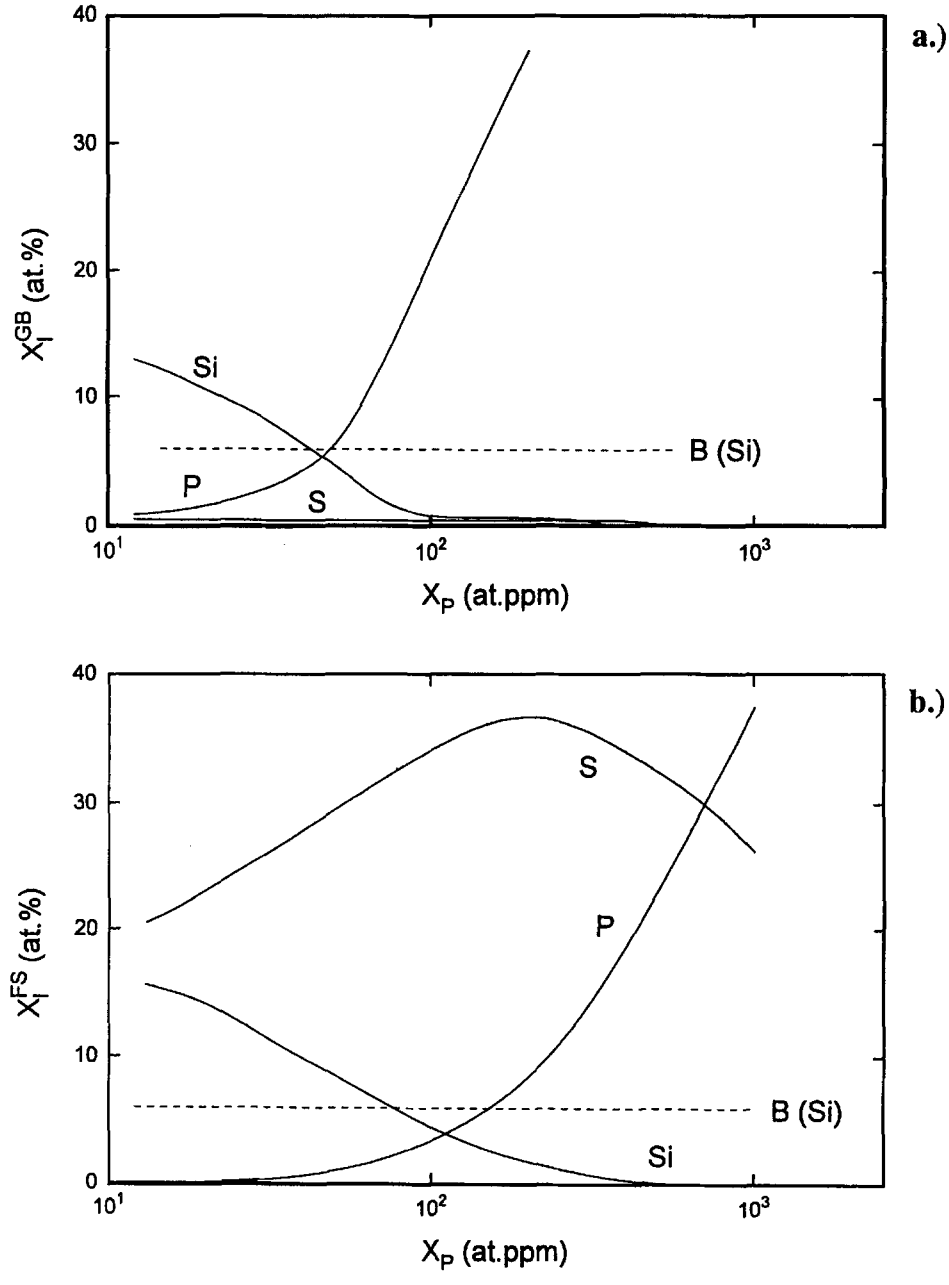

Figure 9. Dependence of the segregation to (a) the {013} grain boundary and (b) the (013) free surface on the bulk content of phosphorus. B(Si) represents the bulk concentration of silicon (6 at.%). The parameters used: $X_S = 17$ at.ppm, $\Delta G^{\circ}_{Si,GB} = -5.5$ kJ/mol, $\Delta G^{\circ}_{P,GB} = -52$ kJ/mol, $\Delta G^{\circ}_{S,GB} = -40$ kJ/mol, $\Delta G^{\circ}_{Si,FS} = -40$ kJ/mol, $\Delta G^{\circ}_{P,GB} = -45$ kJ/mol, $\Delta G^{\circ}_{S,GB} = -75$ kJ/mol, $\alpha'_{SiP} = 92$ kJ/mol, $\alpha'_{SiS} = 38$ kJ/mol, $\alpha'_{PS} = 0$ kJ/mol at 873 K. (After Lejček et al. [88, 89].)

empirically this method by considering the orientation dependence of grain boundary segregation. On the basis of such three-dimensional *grain boundary segregation diagrams* relating grain boundary composition to the bulk solid solubility and to the grain boundary orientation, it should be possible to predict the composition of individual grain boundaries in a given one-matrix base binary system. In contrast to the original method of Seah and Hondros, however, no experimental grain boundary segregation diagram has been constructed since its suggestion in the 1980s. This was probably due to the lack of reliable data resulting from

difficult preparation of oriented bicrystals of various alloys containing well-characterized grain boundaries. Only recently, the set of data obtained by studies on anisotropy of grain boundary segregation of Si, P and C in an α-Fe-Si alloy led to the construction of such diagrams showing the dependences of ΔH_I^0 on both the logarithm of bulk solid solubility and the grain boundary orientation characterized by the deviation angle of the grain boundary plane from the symmetrical position [45, 77] or by the misorientation angle for the symmetrical grain boundaries [46].

A recent thermodynamic analysis of the dependence of segregation enthalpy on bulk solid solubility performed by Lejček and Hofmann [31] allows to express the enthalpy of grain boundary segregation as a function of bulk solid solubility and grain boundary structure by

$$\Delta H_I^0(\Phi, X_I^*) = \Delta H^*(\Phi) + vR[T \ln X_I^*] \qquad (12)$$

According to Eq. (12) the segregation enthalpy, which is a complex function of the interfacial structure and the nature of both matrix and solute, can be expressed as a sum of two independent terms. The first is the segregation enthalpy of a solute with unlimited solubility in a given matrix for a given interface Φ, $\Delta H^*(\Phi)$, which reflects the structural dependence of interfacial segregation. The other is the product $vR[T \ln X_I^*]$ containing both the matrix parameter v relating bulk solute activity a_I^* with atomic ratio X_I^* at the solid solubility limit according to $a_I^* = (X_I^*)^v$, and the term $[T \ln X_I^*]$ which characterizes the bulk system $M-I$ and which is independent of temperature. In fact, Eq. (12) represents an extension of the model of Seah and Hondros [30] by taking additionally into account (i) the structural dependence of interfacial segregation (i.e., $\Delta H^*(\Phi) \neq$ const), and (ii) the non-ideal behavior of the system $M - I$ (i.e., $v \neq 1$). As an example, the grain boundary segregation diagram for the [100] symmetrical tilt grain boundaries is shown in Fig. 10.

Grain boundary segregation diagrams can be used to predict the enthalpy of grain boundary segregation for any element in a given matrix (in our case α-Fe) at individual grain boundaries only on the basis of its solid solubility data. The limitation to a one-matrix systems as compared to the general plot of enrichment ratios against solute solubility of Seah and Hondros follows from different values of the parameter v for different matrices, and from the orientation dependence of $\Delta H^*(\Phi)$ which is not necessarily the same for all possible systems (it is changed e.g., with the crystallography of the matrix). On the other hand, the thermodynamic analysis was made without limitation to a specific interface and therefore, similar segregation diagrams could be constructed for surface or phase boundary segregation with the same value of the parameter v [31].

3. Approach to Equilibrium: Segregation Kinetics

Equilibrium segregation represents the chemical composition of an interface characterized by the minimum free energy of the system. The approach to this equilibrium state is generally called *segregation kinetics*. Segregation kinetics depends on many factors such as temperature and bulk chemical composition. Because of the same approach to equilibrium, i.e., by diffusion from the bulk, the segregation kinetics are similar for both the grain boundaries and the free surfaces. The main differences are that no surface evaporation can occur at internal interfaces and that the supply of segregants comes from two sides of a grain boundary and therefore is twice the value obtained for surface segregation. In contrast to grain boundary segregation, surface segregation kinetics can be studied *in situ*.

3.1. McLean's Approach

The kinetics of grain boundary segregation was first described by McLean [3] by application of Fick's laws for diffusion from two semi-infinite half crystals taking into account a constant enrichment factor $\alpha = X_b(\infty)/X_c$, with the bulk solute concentration X_c and the boundary concentration $X_b(\infty)$ at time $t \to \infty$. With $X_b(0)$ at $t = 0$, this model gives for the time dependence of $X_b(t)$

$$\frac{X_b(t) - X_b(0)}{X_b(\infty) - X_b(0)} = 1 - \exp\left(\frac{4Dt}{\alpha^2 d^2}\right)\left[1 - \operatorname{erf}\left(\frac{4Dt}{\alpha^2 d^2}\right)^{1/2}\right] \qquad (13)$$

where D is the bulk diffusivity and d is the boundary layer thickness.

In general, the approach to equilibrium after the McLean model (Eq. (13)) is too slow because of the oversimplified assumption $\alpha = X_b(\infty)/X_c = \text{const}$, which impedes experimental fits of measured surface segregation data [90, 91]. The reason is that the thermodynamically correct enrichment factor β, as given

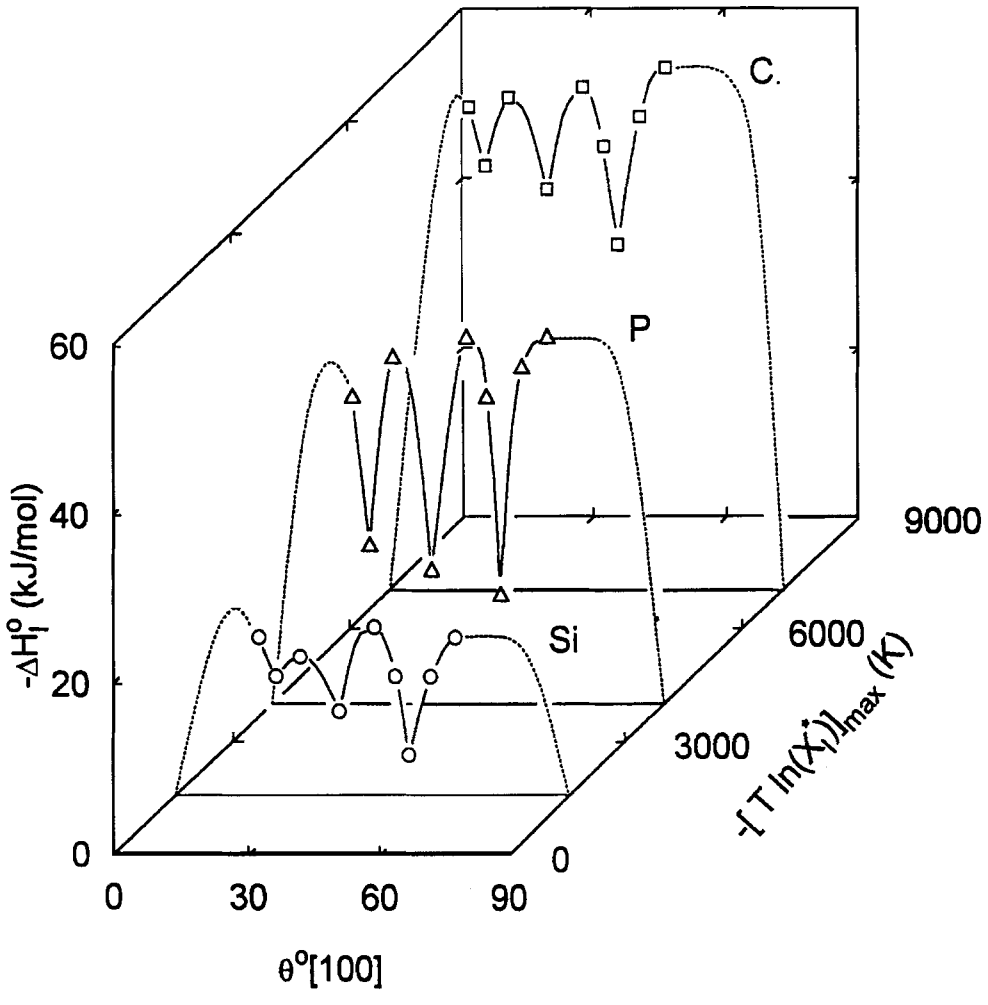

Figure 10. Grain boundary segregation diagram for the [100] symmetrical tilt grain boundaries in α-Fe. (After Lejček and Hofmann [31].)

by Eq. (7), depends on the segregation free energy and usually is higher than α. Consequently, Lea and Seah [91] could only fit their data on surface segregation of Sn in Fe to Eq. (13) by introducing an α varying with $X_b(t)$, for which a detailed analysis was given by Rowlands and Woodruff [92].

3.2. *Ideal Sink Approach*

In order to explain their results of surface segregation of Sn on Cu, Hofmann and Erlewein [90, 93] used an atomic jump model taking into account the segregation free energy ΔG_s, which considerably reduces the atomic jump probability from the segregation layer back to the bulk and therefore works in favor of non-restricted out-diffusion from a semi-infinite bulk. For sufficiently high ΔG_s, the solution is given by

$$\frac{X_b(t) - X_b(0)}{X_b(\infty) - X_b(0)} = X_c \left[1 + \frac{2}{d} \left(\frac{Dt}{\pi} \right)^{1/2} \right] \quad (14)$$

Figure 11 shows the calculated time development for $X_b(t)$ and the adjacent bulk concentration which perfectly fitted the data for Sn on Cu [90, 93]. Only for short times, it can be shown that Eq. (13) also represents a square root dependence of $X_b(t)$ with time, because for any $\alpha > 1$ the first atom transport only stems from the bulk, i.e., the "ideal sink" solution of Eq. (14) applies. With decreasing absolute values of ΔG_s, deviations from Eq. (14) occur as shown in Fig. 11(b). There are many examples of successful application of Eq. (14) in the literature [94–99]. Extensions to ternary systems were given by Tyson [100] incorporating Guttmann's

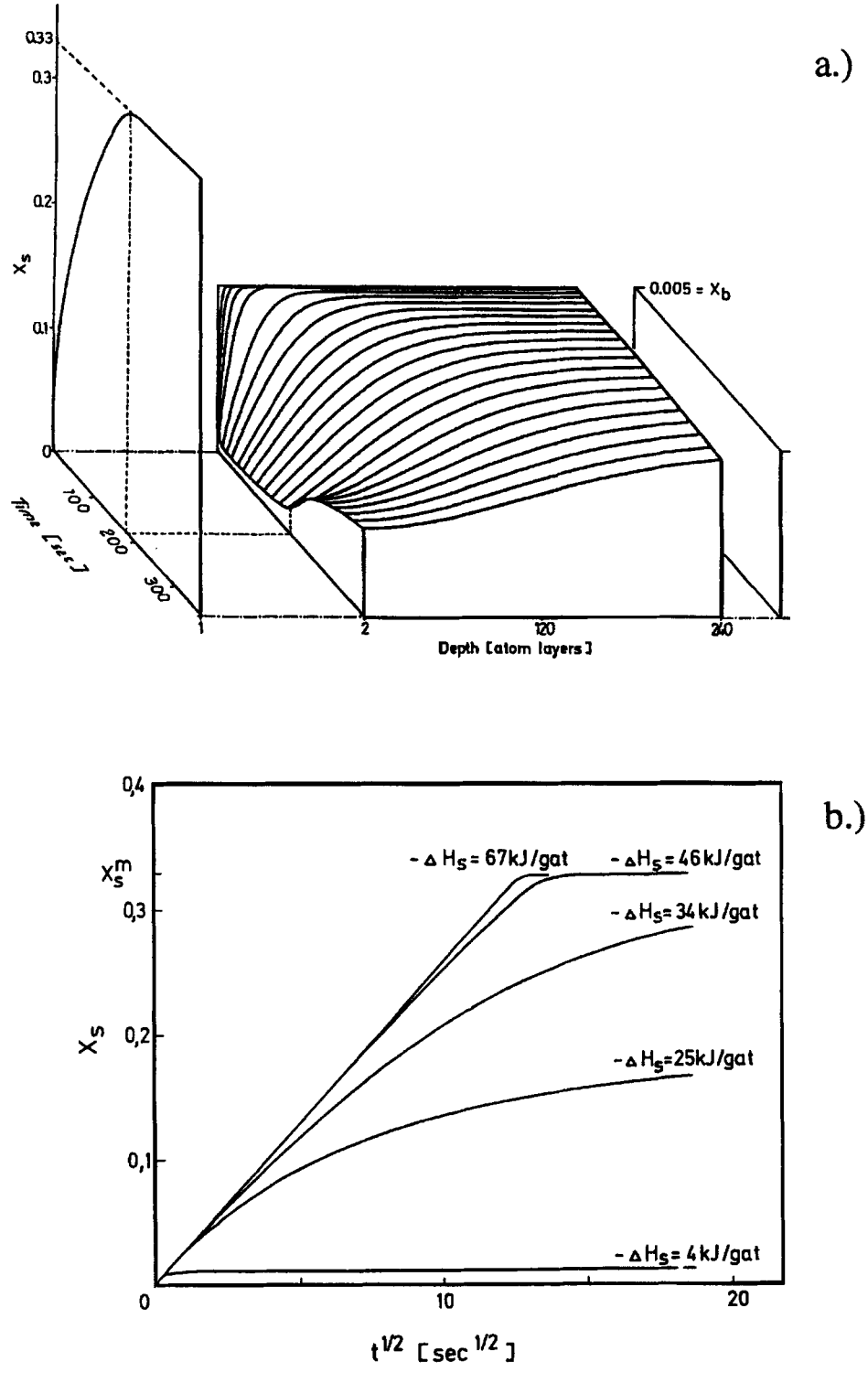

Figure 11. Time dependence of (a) the surface enrichment and subsurface composition distribution of Sn on Cu (0.5 at.% Sn), calculated with the atomic jump model, and (b) the surface concentration showing the onset of deviations from a $t^{1/2}$ low for different segregation free energies ΔG_s. (After Hofmann and Erlewein [93].)

theory of solute segregation, and by Militzer et al. [101–103] considering another diffusion paths such as dislocation pipes. Attainment of true equilibrium conditions is experimentally limited for high temperatures by the quenching rate and for low temperatures by reasonable annealing times.

An estimate of the annealing time t_e needed to approach equilibrium segregation from Eq. (14) gives

$$t_e = \frac{\pi}{D}\left(\frac{X_b(\infty)d}{2X_c}\right)^2 \tag{15}$$

Equation (15) is important for sample preparation in experimental studies of equilibrium grain boundary segregation, yielding a time limit for the lower temperature. On the other hand, there is also a limit for the highest possible temperature which is given by the attainable quenching rate $r = \Delta T/\Delta t$ and temperature T_q with respect to diffusivity D and bulk content of the segregant. Approximately, a relation between r and T_q can be derived following a suggestion of McLean to neglect the transport after $D = D_0 \exp(-Q/RT)$ is diminished by a factor 2, giving

$$\Delta T = \frac{T_q^2}{\left(T_q + \frac{Q}{R\ln 2}\right)} = r\Delta t \tag{16}$$

with

$$\Delta t \approx \left(\frac{\Delta X_b d}{2X_c}\right)^2 \frac{\pi}{D} \tag{17}$$

it follows that

$$r = \frac{T_q^2}{\left(T_q + \frac{Q}{R\ln 2}\right)}\left(\frac{2X_c}{\Delta X_b d}\right)^2 \frac{D_0}{\pi}\exp\left(-\frac{Q}{RT}\right) \tag{18}$$

Equations (16)–(18) represent a rough estimate and may be modified if e.g., vacancy drag to the boundary is additionally considered [28]. A test of the attainment of equilibrium temperature can be made by careful comparison and quantitative evaluation of AES sputter depth profiles at the fracture surface, as shown in Fig. 12 for In segregation at a Ni {115} symmetrical

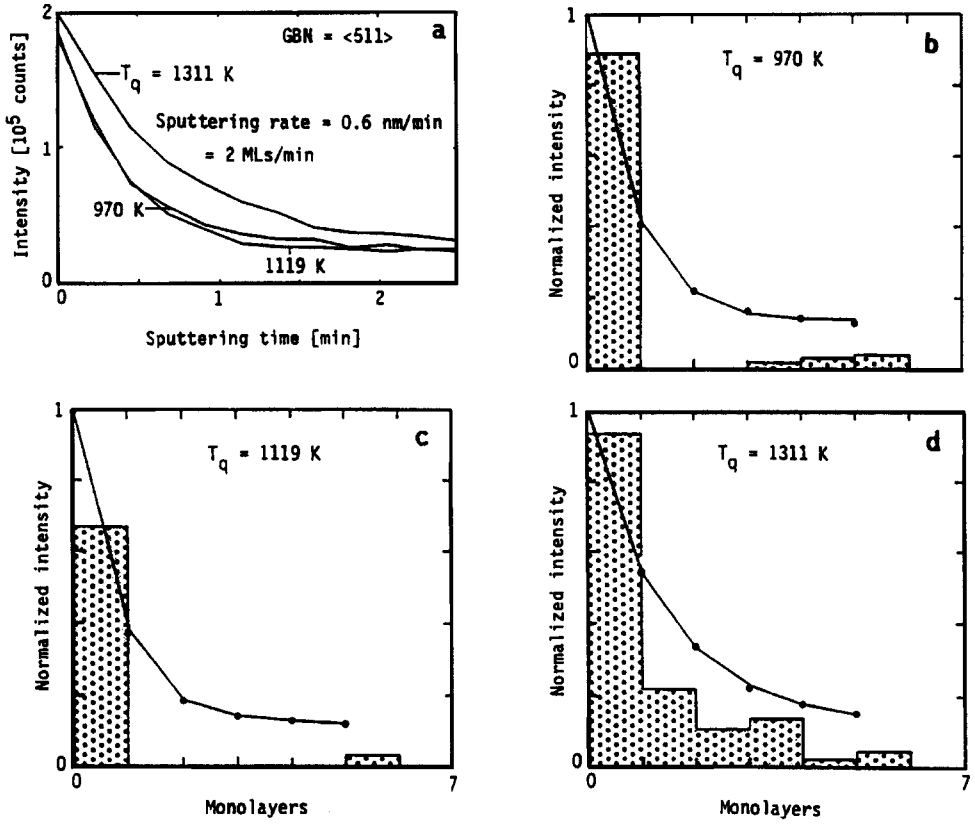

Figure 12. Influence of quench-induced non-equilibrium segregation of In on the shape of AES sputtering profiles and the in-depth distribution of In at the fracture surface of Ni-1.4 at.% In bicrystals quenched from T_q = 970 K, 1119 K and 1311 K. The in-depth distributions (b)–(d) result from the analysis of the In sputtering profiles (a) using the sequential sputtering model. (After Muschik et al. [85].)

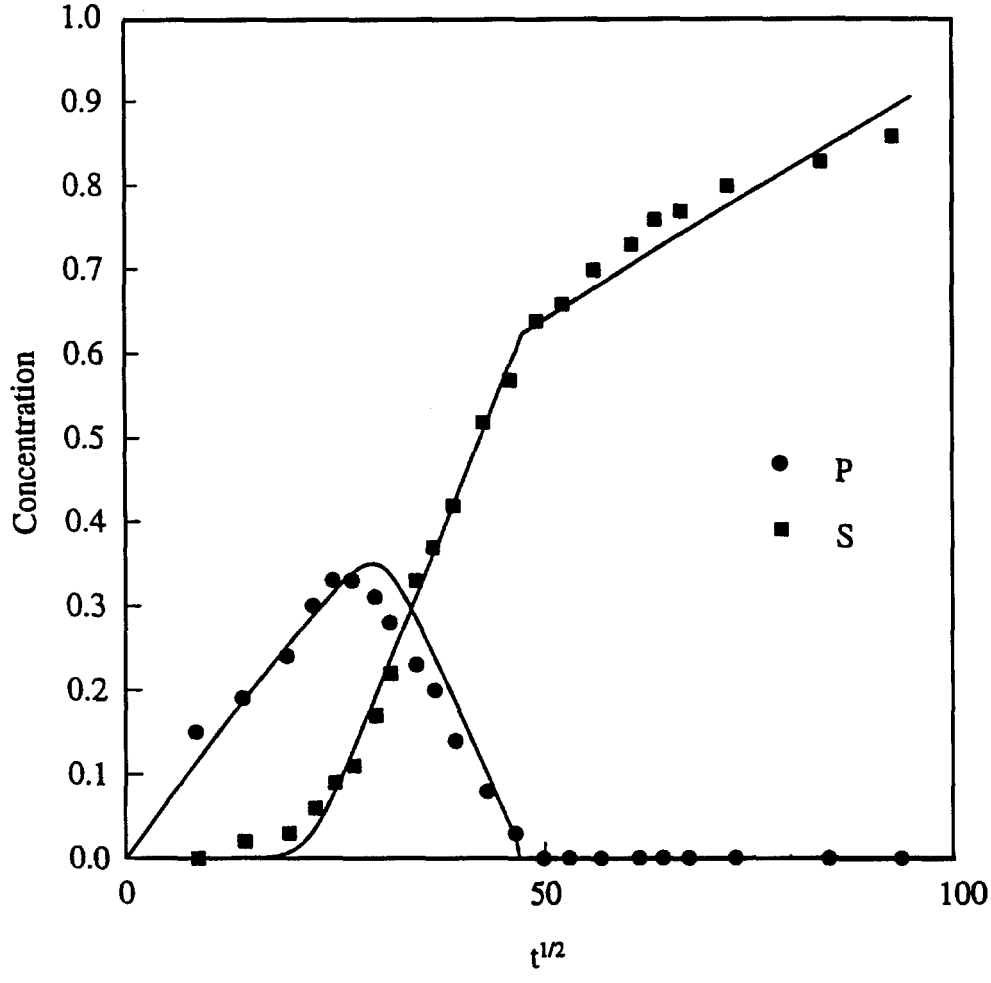

Figure 13. Comparison of measured surface segregation kinetics for P (●) and S (■) in Cu at 943 K and comparison with theoretical calculations (solid lines). (After Militzer and Hofmann [105].)

tilt grain boundary. Evaluation of the in-depth distribution of In disclosed a high amount of In in the region below the first monolayer for a quenching temperature $T_q = 1311$ K which indicates quench-induced non-equilibrium segregation [86].

3.3. *Kinetics of Segregation in Multicomponent Systems*

Similary to equilibrium segregation, grain boundary segregation kinetics is also technically more difficult to measure than surface segregation kinetics (cf., Section 2.5). Therefore, the amount of reliable data is still limited. Directly accessible is the time dependence of surface segregation. Diffusion analysis of observations of the competitive sulfur and phosphorus segregation at a Cu (011) surface was recently elucidated by Militzer and Hofmann [104, 105] as shown in Fig. 13 for $T = 943$ K. Phosphorus with a one order-of-magnitude higher effective diffusivity segregates first to the surface but is replaced by sulfur with the higher segregation enthalpy as soon as it arrives at the surface. In the later stage, the transport of S to the surface is lowered by transition from a $c(2 \times 2)$ to a $p(1 \times 1)$ surface structure which, in combination with the bulk diffusion of P, results in a vanishing flux from the dislocation pipes. A qualitatively similar behavior is expected at grain boundaries, but a direct comparison is impeded by the different segregation enthalpies for the respective elements for this case (cf. Fig. 9).

Lejček et al. [88, 89] made an attempt to measure kinetics of solute segregation to the {013} symmetrical

tilt grain boundary in bicrystal of an Fe-6 at.% Si alloy at 900 K in comparison to the surface segregation kinetics. The starting rapid segregation of silicon was gradually reduced by segregating phosphorus (and carbon in samples containing interstitials) resulting in silicon depletion in equilibrium. This behavior was found qualitatively different from that of a (013) free surface where sulfur segregation was observed to be dominating with increasing time in interstitial-free samples, whereas a strong cosegregation of nitrogen and silicon in samples containing interstitials resulted in formation of a Si_xN_y 2-D surface compound (as clearly indicated by a time evolution of the shift of the Si LVV Auger peak) and suppressed the segregation of other elements. This was already mentioned in Section 2.5. Some indication of non-equilibrium segregation at grain boundaries can be determined e.g., by depth profiling at fracture surfaces [28] which in that case show profiles similar to those in Fig. 11(a) before saturation. A combination of Eqs. (1), (2) and (14) has been shown to predict the temperature–time behavior of temper brittleness as shown for phosphorus in steel by Seah [106].

4. Consequences of Grain Boundary Segregation: Grain Boundary Cohesion and Fracture

Any kind of properties which involve grain boundary energetics and kinetics are influenced by solute segregation. Typical examples are intergranular cohesion and fracture. Recently, appreciable progress has been made in understanding the physical principles and the atomistic mechanisms which are responsible for the observed macroscopic phenomena.

4.1. Grain Boundary Cohesion

The fracture strength of polycrystalline material is mainly governed by the grain boundary cohesion energy. A measure of its decrease by segregation of impurities such as P, As, Sn and Sb which weaken interfacial bond strengths [107], is the shift of the ductile-brittle transition temperature (DBTT) in low alloy steels [100, 106]. Using a simple pair-bonding model, the influence of segregants on the fracture strength of a boundary has been described by Seah [108] in terms of the *broken bond energy* of the elements at the boundary, given by the molar sublimation enthalpy H^{sub} per unit area. In the ideal solution approximation, the change in boundary cohesion energy ΔFE by a segregant A is then roughly determined by the difference of its sublimation enthalpy to that of the matrix B, and proportional to its amount X_b at the grain boundary

$$\Delta FE = \frac{Z_b}{N_0 Z}\left(\frac{H_A^{sub}}{a_A^2} - \frac{H_B^{sub}}{a_B^2}\right) X_b \qquad (19)$$

where N_0 is the Avogadro's number, Z_b and Z are the coordination numbers in the boundary and the bulk, and a_A and a_B are the atomic diameters of solute A and matrix B elements, respectively. Depending on the relative values of ΔH_A^{sub} and ΔH_B^{sub}, ΔFE may be positive or negative, i.e., weaking or strengthening of the boundary may occur. Of course, several solutes can be taken into account in Eq. (19).

Although Eq. (19) does not include thermochemical details of grain boundary bonding and only gives an upper limit for ΔFE if fracture occurs in a completely adiabatic way, excluding relaxation of solute atoms during fracture, it provides a reasonable correlation with measured fracture energies in W(Ni, Fe) sintered samples [109] shown in Fig. 14. Of the segregated elements, Ni, Fe, O, C, determined at the fracture surface by Auger electron spectroscopy (AES), according to Seah [108] only carbon has a strengthening effect. Increasing its amount relative to the other segregants by annealing in CH_4, ΔFE is increased. According to Rice and Wang [110], ΔFE is generaly lowered by an amount of energy released by the relaxation of segregated atoms during fracture. This term, however, in general is small as compared to the main term which is

$$\Delta FE \approx \Gamma_b(\Delta G_s - \Delta G_b) \qquad (20)$$

where Γ_b is the number of solute atoms per boundary area, and ΔG_s and ΔG_b are the surface and grain boundary free segregation enthalpies, respectively. Equation (20) gives again an upper limit and is in close analogy to Eq. (19) [108]. In this way, ΔFE can be obtained from the measured values of ΔG_s and ΔG_b.

Using a technique developed by Muschik et al. [85] to simultaneous measuring the temperature dependence of surface and grain boundary segregation which was described in Section 2.5, Otterbein et al. [38, 87] determined ΔG_s and ΔG_b for B and S in Ni_3Al bicrystals. The results show, in accordance with the prediction after Eq. (19) [108] a decrease of the cohesion energy for S and an increase for B segregation, respectively. The absolute values of ΔFE were found considerably lower than those predicted in [108]. However, in this system the attainment of

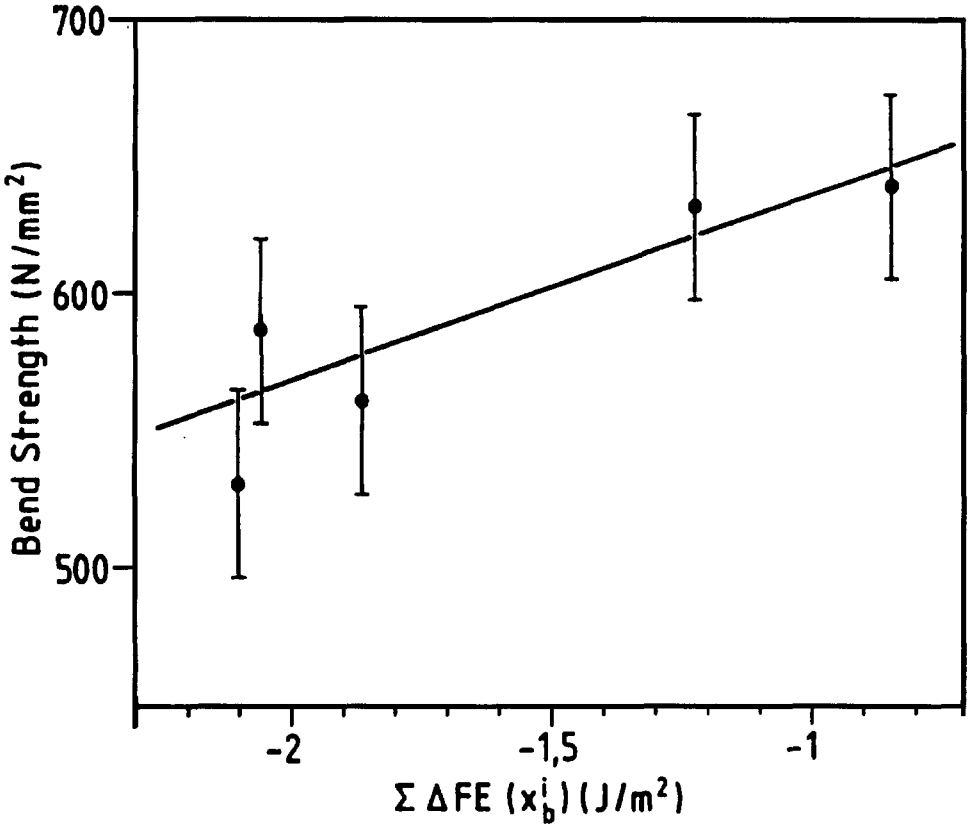

Figure 14. Fracture bend strength of W(Ni, Fe) sintered samples with varying amount of segregation of Ni, Fe, O, and C. In particular, the C content was increased by anneling in a CH_4 atmosphere which resulted in increasing boundary cohesion. $\Sigma\Delta FE(X_i^{gb}) = 1.1X_C^{gb} - [1.8X_{Fe}^{gb} + 1.6X_{Ni}^{gb} + 2.4X_O^{gb} + 3.4X_P^{gb}]$ (J/m^2). (After Hofmann and Hofmann [109].)

segregation equilibrium was difficult and therefore the accuracy of the segregation free enthalpies which is decisive in Eq. (20) was rather limited. As expected, the cohesion energy change correlates with the grain boundary segregation free energy of B and is lower for the $\Sigma = 3$, {111} symmetrical tilt grain boundary ($\Delta G_b = -25$ kJ/mol, $\Delta FE = 36$ mJ/m^2), higher for the $\Sigma = 11$, {113} one ($\Delta G_b = -34$ kJ/mol, $\Delta FE = 106$ mJ/m^2) and maximum for the $\Sigma = 3$, {112}, $\Sigma = 11$, {233} and random boundaries ($\Delta G_b \leq -42$ kJ/mol, $\Delta FE \geq 240$ mJ/m^2).

4.2. *Grain Boundary Fracture*

As was suggested above, segregating atoms produce new bonding relations at grain boundaries. It was found theoretically that strong electronegative metalloids such as phosphorus and sulfur draw charge from the surrounding metallic atoms (e.g., Fe and Ni) at the boundary thus weakening the adjacent metal-metal bonds [107, 111, 112]. As a result, bonding parallel to the boundary is stronger than that perpendicular to the interface. This results in a reduction of cohesion across the boundary and thus, in grain boundary embrittlement. Fracture passes through a metallic material by breaking these weakened metal-metal bonds in the neighborhood of the strong metal-metalloid bonds [113]. In this way the fracture path zigzags along the boundary, and the segregants are distributed between the two newly created fracture surfaces. It is generally supposed that this distribution is homogeneous, i.e., that always one half of the segregated species remains on each fracture surface. This assumption was shown to be correct by several measurements of grain boundary composition on both matching fracture surfaces. For example, Hofmann and Hofmann [109] observed a reasonable agreement between phosphorus concentration on corresponding facets of both matching fracture surfaces of polycrystalline tungsten,

whereas significant differences in its content at different interfaces were observed.

More recent observations performed on grain boundary fracture surfaces of bicrystals showed, however, that the above assumption about homogeneous distribution of segregants between the two fracture surfaces cannot be generally accepted. A detailed study of chemical composition of the two sides of a separated symmetrical {013} grain boundary in an Fe-Si alloy performed by Menyhard et al. [114, 115] revealed markedly different concentrations of phosphorus not only on both matching parts of the broken boundary but even at different areas of a single fracture surface. These differences were explained by the existence of two energetically equivalent fracture paths at both sides of the grain boundary core: After meeting a defect of the grain boundary such as deformation twin [116–118] created at the boundary immediately before cracking at low temperature, the fracture can jump onto the corresponding path on the other side of this symmetrical {013} grain boundary [114, 115]. However, the samples in this study were not equilibriated and therefore, the region of increased phosphorus concentration was relatively wide. Systematic studies of equilibrium segregation characterized by a narrow (one-monolayer-thick) segregation zone in the same system showed that the distribution of segregants is equal in the case of symmetrical grain boundaries [47]. On the other hand, composition of the two fracture surfaces differs systematically in the case of asymmetrical grain boundaries. It is probably due to the asymmetrical distribution of segregated atoms—and thus weakened metal-metal bonds—at an asymmetrical grain boundary [47, 119]. The question of uneven distribution of segregants between the two fracture surfaces of an asymmetrical grain boundary is very important e.g., for quantification of the AES results [120].

5. Conclusions

During the past three decades, a reliable framework of the principles of grain boundary segregation in metallic materials has been developed. Thermodynamics of equilibrium segregation including solute-solute interaction as well as the kinetics of segregation are fairly well understood, and predictions based on thermochemical properties of the respective bulk systems are possible with reasonable precision. Consequently, the influence of segregation on many materials properties can be derived at least semi-quantitatively. Recent progress in experimental studies of the anisotropy of grain boundary segregation in oriented bicrystals resulted in a correlation between thermodynamic and structural aspects through grain boundary segregation diagrams. In the course of these decades we tried to contribute to the basic knowledge of the subject mainly in this field as it is summarized in the present feature article.

Nevertheless, many questions remain open concerning the atomistic aspects of the relationship between grain boundary segregation and structure, and its effect on materials properties. Such questions are, for example, the distribution of energetically different segregation sites in structurally different boundaries of all types, including asymmetrical and mixed ones, the segregation dependent structural changes and faceting, the chemical bonding states of segregants and a full three-dimensional description of grain boundary structure with segregants. Extensions to more complicated cases of heterophase boundaries in thin film structures are not yet fully explored. Recent rapid advance of computational methods evoked extended theoretical modeling of solute atom behavior in a given boundary structure. This effort requires, however, detailed experimental verification. We expect that this verification will be facilitated by further progress in methods with high spatial resolution such as atom-probe field ion microscopy or high-resolution transmission electron microscopy in combination with electron energy loss spectroscopy, favorably applied in combination with the methods of surface analysis (scanning Auger microprobe) and surface probe techniques such as scanning tunneling microscopy and atom force microscopy.

Acknowledgments

Support of the Commission of the European Communities (Contract No. CIPA CT93 0112 (DG 12 HSMU)), the Grant Agency of the Czech Republic (Contract No. 202/94/1177) and the Grant Agency of the Academy of Sciences of the Czech Republic (Contract No. 110404) is gratefully acknowledged.

References

1. E.D. Hondros, M.P. Seah, S. Hofmann, and P. Lejček, in *Physical Metallurgy*, edited by R.W. Cahn and P. Haasen (North Holland, Amsterdam, 1996). 4th ed., p. 1201.
2. P. Lejček and S. Hofmann, Crit. Rev. Sol. State Mater. Sci. **20**, 1 (1995).

3. D. McLean, *Grain Boundaries in Metals* (Clarendon, Oxford, 1957).
4. E.D. Hondros and M.P. Seah, Int. Met. Rev. **22**, 867 (1977).
5. C.J. McMahon, Jr., and L. Marchut, J. Vac. Sci. Technol. **15**, 450 (1978).
6. R.W. Balluffi, in *Interfacial Segregation*, edited by W.C. Johnson and J.M. Blakely (ASM, Metals Park, Ohio, 1979), p. 193.
7. M. Guttmann and D. McLean, in *Interfacial Segregation*, edited by W.C. Johnson and J.M. Blakely (ASM, Metals Park, Ohio, 1979), p. 261.
8. M.P. Seah, J. Phys. F: Metal Phys. **10**, 1043 (1980).
9. E.D. Hondros and M.P. Seah, in *Physical Metallurgy*, 3rd ed., edited by R.W. Cahn and P. Haasen (North Holland, Amsterdam, 1983), p. 855.
10. S. Hofmann, Scann. Electr. Microsc. **III**, 1071 (1985).
11. H.J. Grabke, in *Chemistry and Physics of Fracture*, edited by R.M. Latanision and R.H. Jones (Nijhoff, Dordrecht, 1987), p. 388.
12. S. Hofmann, J. Chim. Phys. **84**, 141 (1987).
13. J. Nowotny, in *Surfaces and Interfaces of Ceramic Materials*, edited by L.-C. Dufour, C. Monty, and G. Petot-Ervas (Kluwer, Dordrecht, 1989), p. 205.
14. M.P. Seah, in *Practical Surface Analysis*, Vol. 1, 2nd ed., edited by D. Briggs and M.P. Seah (John Wiley and Sons, Chichester, 1990), p. 311.
15. S. Hofmann, in *Surface Segregation Phenomena*, edited by P.A. Dowben and A. Miller (CRC Press, Boca Raton, 1990), p. 107.
16. M. Polak, in *Surface Segregation Phenomena*, edited by P.A. Dowben and A. Miller (CRC Press, Boca Raton, 1990), p. 291.
17. J. du Plessis, Sol. State Phenom. **11**, 1 (1990).
18. J. Cabané and F. Cabané, Sol. State Phenom. **15–16**, 1 (1991).
19. C.L. Briant, in *Structure and Property Relationships for Interfaces*, edited by J.L. Walter, A.H. King, and V. Tangri (ASM, Metals Park, 1991), p. 43.
20. R.H. Jones, N.T. Saenz, and C.H. Schilling, in *Structure and Property Relationships for Interfaces*, edited by J.L. Walter, A.H. King, and V. Tangri (ASM, Metals Park, 1991), p. 156.
21. C.L. Briant, in *Materials Interfaces: Atomic-Level Structure and Properties*, edited by D. Wolf and S. Yip (Chapman and Hall, London, 1992), p. 463.
22. C.L. Briant and D.N. Seidman, in *Materials Interfaces: Atomic-Level Structure and Properties*, edited by D. Wolf and S. Yip (Chapman and Hall, London, 1992), p. 497.
23. A.P. Sutton and R.W. Balluffi, *Interfaces in Crystalline Materials*, (Clarendon, Oxford, 1995).
24. E.D. Hondros and M.P. Seah, Metall. Trans. **8A**, 1363 (1977).
25. P. Lejček, Int. J. Modern Phys. B **7**, C1-179 (1990).
26. K. Lösch, Ph.D. Thesis (University Stuttgart, 1987).
27. T. Muschik, Ph.D. Thesis (University Stuttgart, 1988).
28. T. Muschik, W. Gust, S. Hofmann, and B. Predel, Acta Metall. **37**, 2917 (1989).
29. S. Hofmann and P. Lejček, J. Phys. France **51**, C1-179 (1990).
30. M.P. Seah and E.D. Hondros, Proc. Roy. Soc. A **335**, 191 (1973).
31. P. Lejček and S. Hofmann, Interface Sci. **1**, 163 (1993).
32. R.H. Fowler and E.A. Guggenheim, *Statistical Thermodynamics* (Cambridge University Press, Cambridge, 1939).
33. C. Pichard, M. Guttmann, J. Rieux, and C. Goux, J. Phys. France **36**, C4-151 (1975).
34. M. Menyhard, B. Blum, and C.J. McMahon, Jr., Acta Metall. **37**, 549 (1989).
35. R. Herschitz and D.N. Seidman, J. Phys. France **46**, C4-451 (1985).
36. M. Militzer and J. Wieting, Acta Metall. **35**, 2765 (1987).
37. S. Hofmann and H. Hofmann, J. Phys. France **46**, C4-633 (1985).
38. U. Otterbein, Ph.D. Thesis (University Stuttgart, 1994).
39. P. Lejček and S. Hofmann, Surf. Interface Anal. **16**, 546 (1991).
40. P. Gas, M. Guttmann, and J. Bernardini, Acta Metall. **30**, 1309 (1982).
41. C.L. Briant, Mater. Sci. Technol. **4**, 956 (1988).
42. C.L. Briant, Metall. Trans. **21A**, 2339 (1990).
43. A. Biedermann, M. Schmid, B.M. Reichl, and P. Varga, Fres. J. Anal. Chim. **353**, 259 (1995).
44. P. Lejček and S. Hofmann, Acta Metall. Mater. **39**, 2469 (1991).
45. P. Lejček, J. Adámek, and S. Hofmann, Surface Sci. **264**, 449 (1992).
46. S. Hofmann, P. Lejček, and J. Adámek, Surf. Interface Anal. **19**, 601 (1992).
47. P. Lejček, Anal. Chim. Acta **297**, 165 (1994).
48. K. Masuda-Jindo, Phys. Stat. Sol. (b) **134**, 545 (1986).
49. M.P. Seah and C. Lea, Philos. Mag. **31**, 627 (1973).
50. H. Hänsel and H.J. Grabke, Scripta Metall. **20**, 1641 (1986).
51. H. Erhart and H.J. Grabke, Metal Sci. **15**, 401 (1981).
52. K. Tatsumi, N. Okumura, and S. Funaki, in *Proc. JIMIS-4 "Grain Boundary Structure and Related Phenomena"*. Trans JIM (Suppl.) (1986), p. 427.
53. P. Lejček, Mater. Sci. Eng. A **185**, 109 (1994).
54. C.L. White and W.A. Coghlan, Metall. Trans. **8A**, 1403 (1977).
55. C.L. White and D.F. Stein, Metall. Trans. **9A**, 13 (1978).
56. M. Menyhard and C.J. McMahon, Jr., Acta Metall. **37**, 2287 (1989).
57. M.A. Hoffmann and P. Wynblatt, Metall. Trans. A **20**, 215 (1989).
58. V. Paidar, A. Machová, and V. Vejvalková, Modelling Simul. Mater. Sci. Eng. **2**, 1131 (1994).
59. P. Lejček, Prog. Surface Sci. **35**, 209 (1990).
60. H.F. Fischmeister, J. Phys. France **46**, C4-3 (1985).
61. W.R. Thomas and B. Chalmers, Acta Metall. **3**, 17 (1955).
62. T. Watanabe, S. Kitamura, and S. Karashima, Acta Metall. **28**, 455 (1980).
63. T. Watanabe, J. Phys. France **46**, C4-555 (1985).
64. M. Biscondi, J. Phys. France **43**, C6-293 (1982).
65. B.W. Krakauer and D.N. Seidman, Mater. Sci. Forum **126–128**, 161 (1993).
66. T. Watanabe, T. Murakami, and S. Karashima, Scripta Metall. **12**, 361 (1978).
67. J.P. Hirth and J. Lothe, *Theory of Dislocation* (Wiley, New York, 2nd ed., 1982).
68. A. Fraczkiewicz and M. Biscondi, J. Phys. France **46**, C4-497 (1985).
69. J. Stolarz and J. Le Coze, J. Phys. France **51**, C1-641 (1990).
70. D.N. Seidman, Mater. Sci. Eng. A **137**, 57 (1991).
71. J.G. Hu and D.N. Seidman, Scripta Metall. Mater. **27**, 693 (1992).
72. B.W. Krakauer and D.N. Seidman, Mater. Sci. Forum **154–156**, 189 (1994).
73. S. Suzuki, K. Abiko, and H. Kimura, Scripta Metall. **15**, 1139 (1981).

74. D. Bouchet and L. Priester, Scripta Metall. **20**, 961 (1986).
75. D. Bouchet and L. Priester, Scripta Metall. **21**, 475 (1987).
76. D. Wolf, J. Phys. France **46**, C 1-197 (1985).
77. S. Hofmann and P. Lejček, Scripta Metall. Mater. **25**, 2259 (1991).
78. P. Lejček and S. Hofmann, Mater. Sci. Forum **126–128**, 157 (1993).
79. V. Paidar, Acta Metall. **35**, 2035 (1987).
80. V. Paidar, Philos. Mag. A **66**, 41 (1992).
81. M.P. Seah and C. Lea, Philos. Mag. **31**, 627 (1975).
82. M. Tvrdý, R. Seidl, L. Hyspecká, and K. Mazanec, Scripta Metall. **19**, 51 (1985).
83. D. Alaoua, A. Larère, S. Lartigue, and L. Priester, Mater. Sci. Forum **126–128**, 185 (1993).
84. J. Bernardini, F. Cabané, and J. Cabané, Surface Sci. **162**, 519 (1985).
85. T. Muschik, S. Hofmann, and W. Gust, Scripta Metall. **22**, 349 (1987).
86. T. Muschik, S. Hofmann, W. Gust, and B. Predel, Appl. Surf. Sci. **37**, 449 (1989).
87. U. Otterbein, S. Hofmann, and M. Rühle, MRS Symp. Proc. **288**, 183 (1993).
88. P. Lejček, A.V. Krajnikov, Yu.N. Ivashchenko, M. Militzer, and J. Adámek, Surface Sci. **280**, 325 (1993).
89. P. Lejček, A.V. Krajnikov, Yu. N. Ivashchenko, and J. Adámek, Surface Sci. **269–270**, 1147 (1992).
90. S. Hofmann and J. Erlewein, Scripta Metall. **10**, 857 (1976).
91. C. Lea and M.P. Seah, Philos. Mag. **35**, 213 (1977).
92. G. Rowlands and D.P. Woodruff, Philos. Mag. A **40**, 459 (1979).
93. S. Hofmann and J. Erlewein, Surface Sci. **77**, 591 (1978).
94. G.L.P. Berning and W.J. Coleman, Surface Sci. **173**, 411 (1986).
95. J. du Plessis and P.E. Viljoen, Surface Sci. **131**, 131 (1983).
96. S. Hofmann, Mater. Sci. Eng. **42**, 55 (1980).
97. K. Henessen, H. Keller, and H. Viefhaus,. Scripta Metall. **18**, 1319 (1984).
98. E.C. Viljoen and J. du Plessis, Surf. Interface Anal. **23**, 110 (1995).
99. G. Luckman, in *Auger Electron Spectroscopy*, edited by C.L. Briant and R.P. Messmer (Academic Press, Boston, 1988), p. 17.
100. W.R. Tyson, Acta Metall. **26**, 1471 (1978).
101. M. Militzer and J. Wieting, Acta Metall. **34**, 1229 (1986).
102. M. Militzer, Yu.N. Ivashchenko, A.V. Krajnikov, P. Lejček, and J. Wieting, Prog. Surf. Sci. **35**, 205 (1991).
103. M. Militzer, Yu.N. Ivashchenko, A.V. Krajnikov, P. Lejček, J. Wieting, and S.A. Firstov, Surface Sci. **261**, 267 (1992).
104. M. Militzer and S. Hofmann, Scripta Metall. Mater. **31**, 1501 (1994).
105. M. Militzer and S. Hofmann, J. Vac. Sci. Technol. A **13**, 1493 (1995).
106. M.P. Seah, Acta Metall. **30**, 345 (1977).
107. C.L. Briant and R.P. Messmer, Acta Metall. **30**, 1811 (1982).
108. M.P. Seah, Acta Metall. **28**, 955 (1980).
109. H. Hofmann and S. Hofmann, Scripta Metall. **18**, 77 (1984).
110. J.R. Rice and J.-S. Wang, Mat. Sci. Eng. A **107**, 23 (1989).
111. G.L. Krasko and G.B. Olson, Sol. State Commun. **76**, 247 (1990).
112. R. Wu, A.J. Freeman, and G.B. Olson, J. Mater. Res. **7**, 2403 (1992).
113. W. Losch, in *Chemistry and Physics of Fracture*, edited by R.M. Latanision and R.H. Jones (Nijhoff, Dordrecht, 1987), p. 461.
114. M. Menyhard, C.J. McMahon, Jr., P. Lejček, and V. Paidar, in *Interfacial Structure, Properties and Design*, edited by M.H. Yoo, W.A.T. Clark, and C.L. Briant (MRS, Pittsburgh, 1989). MRS Symp. Proc. **122**, 255 (1989).
115. M. Menyhard, B. Rothman, C.J. McMahon, Jr., P. Lejček, and V. Paidar, Acta Metall. Mater. **39**, 1289 (1991).
116. P. Lejček, J. Brádler, V. Paidar, and M. Koutník, J. Mater. Sci. **22**, 3974 (1987).
117. P. Lejček and S. Hofmann, J. Mater. Sci. Lett. **7**, 646 (1988).
118. P. Lejček, J. Brádler, M. Koutník, V. Paidar, and A. Potměšilová, Appl. Surf. Sci. **44**, 75 (1990).
119. P. Lejček and S. Hofmann, Surface Sci. **307–309**, 798 (1994).
120. P. Lejček and S. Hofmann, in *Proc. ECASIA'95* (Wiley, Chichester, 1996). In press.